SEMMELWEIS EGYETEM

DOKTORI ISKOLA

Ph.D. értekezések

3374.

UJVÁRI ADRIENN

Szív- és érrendszeri betegségek élettana és klinikuma

című program

Programvezető: Dr. Merkely Béla, egyetemi tanár

Témavezető: Dr. Kovács Attila, egyetemi docens

CHARACTERIZATION OF THE PHYSIOLOGICAL PHENOTYPES OF RIGHT VENTRICULAR CONTRACTION

PhD thesis

Adrienn Ujvári MD

Semmelweis University Doctoral School

Cardiovascular Medicine and Research Division

Supervisor: Attila Kovács MD, Ph.D.

Official reviewers: Tamás Horváth MD Ph.D., Viktor József Horváth MD Ph.D.

Head of the Complex Examination Committee: Henriette Farkas MD, Ph.D.

Members of the Complex Examination Committee: Péter Andréka MD, Ph.D., András Vereckei MD, Ph.D.

Budapest
2025

TABLE OF CONTENTS

LIST OF ABBREVIATIONS

2D – two-dimensional

3D – three-dimensional

3DE – 3D echocardiography

A – late diastolic mitral inflow velocity

a′ – peak late (atrial) diastolic annular velocity

ANOVA – analysis of variance

AEF – anteroposterior ejection fraction

AEFi – anteroposterior ejection fraction index

ASE – American Society of Echocardiography

AV – atrioventricular

BMI – body mass index

BSA – body surface area

CEFi – circumferential ejection fraction index

CMR – cardiac magnetic resonance imaging

CO – cardiac output

CPET – cardiopulmonary exercise testing

DBP – diastolic blood pressure

DT – deceleration time

E – early mitral inflow velocity

e′ – early diastolic annular velocity

ECG – electrocardiography

EDA – end-diastolic area

EDVi – end-diastolic volume index

EF – ejection fraction

ESA – end-systolic area

ESVi – end-systolic volume index

FAC – fractional area change

FWLS – free wall longitudinal strain

GAS – global area strain

GCS – global circumferential strain

GLS – global longitudinal strain

HF – heart failure

HR – heart rate

ICC – intraclass correlation coefficients

IVSd – interventricular septal thickness at end-diastole

LAVi – left atrial volume index

LEF – longitudinal ejection fraction

LEFi – longitudinal ejection fraction index

LV – left ventricle

LVIDd – LV internal diameter at end-diastole

LV M – left ventricular muscle mass

LV Mi – left ventricular muscle mass index

PASP – pulmonary artery systolic pressure

PWd – posterior wall thickness at end-diastole

RAVi – right atrial volume index

REF – radial ejection fraction

REFi – radial ejection fraction index

RER – respiratory exchange ratio

RV – right ventricle

RVSP – right ventricular systolic pressure

RWT – relative wall thickness

s′ – systolic annular velocity

SBP – systolic blood pressure

SD – standard deviation

SVi – stroke volume index

TAPSE – tricuspid annular plane systolic excursion

TDI – tissue Doppler imaging

TTE – transthoracic echocardiography

VO_2 – peak oxygen uptake

VO_2/kg – peak oxygen uptake indexed to body weight

1. INTRODUCTION

1.1. The right ventricle

There is a growing recognition of the pivotal role of the right ventricle (RV) in determining functional status and prognosis across a wide range of clinical conditions. The RV differs from the left ventricle (LV) both anatomically and functionally, which limits the direct extrapolation of our understanding of left-sided pathophysiology to the right heart. For decades, the significance of the RV was underappreciated. However, accumulating evidence highlights its nearly universal clinical relevance in settings such as ischemic and nonischemic heart failure (HF)—whether with reduced or preserved ejection fraction (EF)—myocardial infarction, pulmonary hypertension, congenital heart disease, and post-interventional states. For example, RV dysfunction is present in approximately 50% of patients with HF and reduced LV EF, and in about 33% of those with preserved EF. Regardless of LV function, RV dysfunction doubles the risk of HF-related hospital readmissions (1, 2). Based on the prevalence of HF and pulmonary hypertension alone, it is estimated that 400–800 million individuals worldwide may be affected by RV dysfunction, the majority of whom remain undiagnosed (2). Furthermore, accurate assessment of RV morphology and function is critical in pediatric and adolescent cardiovascular disease, particularly in complex congenital heart conditions involving systemic RV physiology (3, 4, 5), obstructive right-sided heart disease (6, 7), and pulmonary hypertension (8, 9). While tools and techniques for assessing the LV are well-established, evaluation of the RV using two-dimensional (2D) echocardiography remains challenging due to its complex anatomy and contraction patterns. However, advancements in three-dimensional echocardiography (3DE) now offer accurate quantification of RV volumes, with validation against gold-standard modalities such as cardiac magnetic resonance (CMR) imaging—even in pediatric patients with complex congenital heart disease.

1.1.1. The anatomy and myoarchitecture of the right ventricle

The RV is a thin-walled, crescent-shaped structure that wraps around the LV, from which it is separated by the interventricular septum. It can be subdivided into anterior, lateral, and inferior walls, as well as basal, mid, and apical segments (10). Anatomically, the RV

is typically described in terms of three main components: the inlet, which includes the tricuspid valve, tendinous chords, and papillary muscles; the trabeculated apex; and the outlet or infundibulum (also known as the conus), a tubular muscular structure that supports the pulmonary valve leaflets. The RV is both morphologically and functionally distinct from the LV. Key distinguishing features of the morphologic RV include uniformly coarse trabeculations—which represent the most consistent anatomical feature for cardiac morphologists—multiple papillary muscles, the presence of a moderator band, and a tri-leaflet atrioventricular (AV) valve with a septal leaflet that is apically displaced relative to the anterior mitral leaflet. Additionally, the RV features a fully muscular outflow tract, in contrast to the aortomitral continuity seen in the LV (11).

The ventricles are composed of multiple layers that form a three-dimensional (3D) network of myocardial fibers (12). The RV wall consists primarily of superficial and deep layers of muscle. The superficial muscle fibers are oriented predominantly in a circumferential direction, running parallel to the AV groove (12, 13). These fibers curve obliquely towards the cardiac apex and extend into the superficial myofibers of the LV (12, 13). In contrast, the deep muscle fibers of the RV are aligned longitudinally from base to apex. The LV exhibits a more complex fiber architecture, with superficial myofibers oriented obliquely, subendocardial fibers aligned longitudinally, and an intermediate layer of predominantly circular fibers. This structural organization underlies the LV's intricate contraction mechanics, including torsion, translation, rotation, and wall thickening (12, 13). Importantly, the continuity between RV and LV muscle fibers functionally links the two ventricles. This connection forms the anatomical basis for free wall traction of the RV during LV contraction and contributes to ventricular interdependence—an interaction further reinforced by the interventricular septum and the pericardium (13).

1.1.2. The development and maturational changes of the right ventricle

Significant transformations occur in the RV throughout aging, particularly after birth and during infancy. In fetal life, several key factors define cardiovascular physiology: high-resistance pulmonary circulation, low-resistance systemic circulation, a large nonrestrictive ductus arteriosus, right-to-left shunting through the foramen ovale, equal pulmonary arterial and aortic pressures, and a state of hypoxemia (14, 15, 16). During

this period, the thickness of the RV and LV free walls, as well as their force-generating capacity, are comparable. The interventricular septum remains midline and flat throughout the cardiac cycle (10). Following birth, RV hypertrophy regresses during infancy, and the heart remodels into the typical postnatal configuration, with a crescent-shaped RV and an elliptically shaped LV. As aging progresses, both the RV and the pulmonary vascular system undergo further changes. Pulmonary artery pressure and vascular resistance tend to increase modestly with age, likely due to progressive stiffening of the pulmonary vasculature (17, 18). Despite these changes, RV and LV EF are generally well preserved during normal aging. However, RV diastolic function shows age-related alterations. Doppler-based flow indices demonstrate reduced early diastolic filling, increased late filling, and decreased myocardial diastolic velocities—patterns that closely parallel the age-associated changes observed in LV diastolic function (19).

Beyond general age-related trends, maturational changes significantly influence the specific mechanics of RV contraction. During the first year of life, the dominant RV contraction pattern shifts from primarily radial contraction to one that is more longitudinally driven. This transition corresponds with a decrease in pulmonary vascular resistance and changes in RV loading conditions. Tricuspid annular plane systolic excursion (TAPSE) and other echocardiographic indices demonstrate an increase in longitudinal contraction during early infancy, followed by stabilization throughout later childhood (20). In addition, anteroposterior contraction—often underrecognized in conventional assessments—contributes substantially to overall RV function and is closely interrelated with LV mechanics. The relative contributions of radial, longitudinal, and anteroposterior components of RV contraction continue to evolve with age, underscoring the importance of age-specific evaluation when assessing RV performance (21).

1.1.3. Contraction pattern of the right ventricle

The RV demonstrates a distinctive, peristaltic-like contraction pattern, in which mechanical activation begins at the inlet and progresses toward the infundibulum (22). During isovolumic contraction, the subepicardial layer of the inflow tract acts as an early pressure generator, contributing to circumferential deformation of the RV. In contrast, subendocardial fibers predominantly initiate longitudinal shortening, particularly during

the ejection phase (23). The interventricular septum also plays a critical role in global RV function, mainly through longitudinal shortening, although it may also exhibit inward motion into the RV cavity. Importantly, the twisting motion of the RV does not significantly contribute to its pump function (24).

Three primary mechanisms contribute to RV contraction: (1) longitudinal shortening, characterized by the apical displacement of the tricuspid annulus; (2) inward (radial) movement of the free wall, commonly referred to as the “bellows effect”; and (3) bulging of the interventricular septum into the RV during left ventricular contraction, which stretches the RV free wall over the septum and results in anteroposterior shortening.

1.1.4. Echocardiographic assessment of right ventricular function

Accurate assessment of RV function is a critical component of every transthoracic echocardiographic (TTE) examination and plays an essential role in the diagnosis and management of a wide range of diseases and conditions. However, evaluating RV function via TTE remains challenging due to the RV's complex geometry. Current guidelines recommend incorporating at least one quantitative parameter in addition to visual assessment (25). Several studies have highlighted the usefulness of various metrics, including TAPSE (26, 27, 28), tissue Doppler imaging of the basal free lateral wall (s′) (29), global longitudinal strain of the RV free wall (RV-GLS) (30, 31, 32), and fractional area change (FAC) (33, 34, 35, 36). Additionally, 3DE offers a highly accurate and reproducible method for quantifying RV volumes and EF (37, 38, 39, 40). TAPSE and s′ primarily assess longitudinal motion of the basal segments of the RV lateral free wall. FAC provides a quantitative measure of area change during systole in the apical four-chamber view. RV-GLS evaluates myocardial deformation, allowing for both regional and global analysis of the RV free wall. Three-dimensional volumetric assessment enables precise quantification of end-diastolic and end-systolic volumes, EF, and stroke volume, and is less influenced by regional variations in RV contractility or passive cardiac motion. Moreover, a novel method called ReVISION (Right VentrIcular Separate wall motIon quantificatiON) has been introduced, offering new insights into both global and segmental RV function by defining parameters that may be more sensitive and predictive than conventional echocardiographic indices (41). The ReVISION technique, based on

3DE data, isolates and quantifies distinct components of RV contraction—longitudinal, radial, and anteroposterior—allowing for a more nuanced evaluation of RV mechanics. By addressing the limitations of traditional parameters such as TAPSE and FAC, which predominantly reflect only single aspects of RV performance, ReVISION provides a more comprehensive analysis of RV contraction patterns. This enhanced characterization may improve the understanding, diagnosis, and management of RV dysfunction in conditions such as congenital heart disease, pulmonary hypertension, and other pathologies.

1.2. Knowledge gaps in the understanding of physiological right ventricular function

1.2.1. Lack of normative values in adults and in the young

Echocardiography plays a pivotal role in the evaluation of cardiac structure and function; however, its diagnostic accuracy depends heavily on the availability of reliable normative reference values. Establishing such reference values is essential for distinguishing physiological variation from pathological findings. Despite this need, significant gaps persist in defining comprehensive normal ranges, particularly across different age groups, including children, adolescents, and athletes. Current echocardiographic guidelines are primarily based on normative data derived from studies focused on adult populations. In adults, recommendations from the American Society of Echocardiography (ASE)(42) and the European Association of Cardiovascular Imaging (EACVI)(43) provide reference ranges for left and right ventricular size, function, and strain measurements. These values are essential for diagnosing conditions such as HF, valvular disease, and pulmonary hypertension. However, there is a lack of robust normative data derived from advanced echocardiographic methods, like 3DE. In pediatric populations, the availability of normative values is even more constrained. Ongoing growth and developmental changes introduce dynamic alterations in cardiac size and function, complicating the establishment of stable reference ranges. To address this, the ASE recently issued updated pediatric echocardiographic guidelines (44), aiming to standardize assessments and provide age-specific normative values. Nevertheless, these guidelines incorporate advanced echocardiographic modalities, such as 3DE, only to a limited extent, highlighting an ongoing need for further research and standardization in this area.

The World Alliance of Societies of Echocardiography (WASE) study(45) has been a significant step in addressing this gap. By compiling data from a diverse, multinational cohort, WASE aims to establish population-specific yet globally applicable echocardiographic reference values. This approach allows for the inclusion of racial, ethnic, and geographic variability in cardiac structure and function, thereby enhancing the precision and universality of echocardiographic interpretation. The findings from WASE have significantly advanced our understanding of how normative cardiac dimensions and function differ across populations, ultimately contributing to more informed and individualized clinical decision-making. However, it is important to note that WASE did not include healthy pediatric populations or athletes, leaving these important subgroups underrepresented in the dataset.

Another critical area in need of standardized normative values is the echocardiographic assessment of athletes. Regular intensive training leads to a series of physiological cardiac adaptations—collectively referred to as the athlete's heart—which include increased chamber dimensions, augmented diastolic function, and altered myocardial strain patterns (46). However, distinguishing these benign adaptations from pathological conditions such as hypertrophic cardiomyopathy or arrhythmogenic cardiomyopathy remains a significant clinical challenge, largely due to the absence of well-defined reference ranges stratified by type and intensity of athletic training. The current lack of sport-specific normative data hampers the accurate interpretation of echocardiographic findings in athletes, thereby increasing the risk of both overdiagnosis and inappropriate exclusion from athletic participation. Establishing robust, sport- and performance-level-specific reference values is essential for improving diagnostic accuracy and ensuring safe, evidence-based decision-making in sports cardiology.

1.2.2. Physiological cardiac remodeling in response to exercise – athlete's heart

The cardiovascular system is subjected to significant hemodynamic demands during high-intensity exercise, which can vary considerably across different sports disciplines. In response, athletes undergo complex structural and functional cardiac adaptations aimed at optimizing performance and sustaining the physiological load imposed by exercise. This phenomenon, commonly referred to as exercise-induced cardiac remodeling or the

athlete's heart, was first characterized in one of the seminal studies by Morganroth et al (47). Cardiac adaptation differs based on the predominant type of exercise—whether primarily isometric or isotonic in nature. Dynamic (isotonic) exercise, such as endurance training, leads to a marked increase in cardiac output (CO), resulting in pronounced dilation of all four cardiac chambers. In contrast, static (isometric) exercise, such as strength training, is associated with increased peripheral vascular resistance and relatively stable or modestly elevated CO, which primarily induces an increase in left ventricular muscle mass (LV M) (47, 48, 49). However, most sports involve varying degrees of both dynamic and static components. Mitchell et al. have argued against a rigid dichotomy, instead recommending classification based on the combined isometric and isotonic demands of each activity. Current guidelines further support this approach by categorizing sports into broader groups—such as skill, power, mixed, or endurance disciplines—to better reflect the diverse physiological demands placed on the cardiovascular system (50, 51).

Extending this concept, it has become increasingly evident that, in addition to the LV, the RV also undergoes marked structural and functional adaptations in response to sustained volume and pressure overload associated with high-intensity endurance training. In response to intensive exercise, the RV undergoes significant volumetric enlargement, with resting RV EF being mildly but consistently reduced compared to sedentary individuals (52, 53). This adaptation reflects a disproportionate pressure and volume load on the RV relative to the LV, resulting in more pronounced RV remodeling (54). Notably, both LV and RV volumes correlate strongly with peak oxygen uptake (VO_2) measured by spiroergometry, underscoring their role in determining exercise capacity (55). These changes are generally considered physiological in elite athletes, though distinguishing them from pathological conditions remains clinically important.

1.2.3. The importance of the young athlete's heart

A deeper understanding and interpretation of distinct contraction patterns may provide an opportunity for more precise insights into cardiovascular physiology, particularly regarding the physiological adaptation of the right heart. Although the 3D deformation of the athlete's heart—especially in terms of RV mechanics—has been scarcely characterized, such analysis may enhance our understanding of the associations between

resting cardiac function and athletic performance. In our research, we aimed to develop a methodology that enables this level of interpretation by examining healthy adults and analyzing the results. Additionally, the study was extended to minors and elite athletes to explore age- and performance-related variations in RV mechanics. This approach may contribute to a clearer distinction between physiological adaptation and pathological remodeling in various athletic and developmental populations.

This topic holds particular significance in a unique and vulnerable population—young elite athletes—who experience the simultaneous influence of two major physiological processes: the substantial cardiovascular changes associated with growth and maturation, and the intense adaptive responses to high-level physical training. Together, these factors drive a complex and dynamic remodeling process that, in most cases, reflects beneficial physiological adaptation. However, the clinical challenge lies in accurately distinguishing these adaptive changes from pathological remodeling. In certain instances, maladaptive changes may increase the risk of arrhythmias, myocardial dysfunction, or even sudden cardiac events. Therefore, a nuanced understanding of age-specific and training-related cardiac adaptations is critical to ensure both the safety and optimal performance of young athletes

Screening young athletes is essential for the early detection of conditions that may predispose them to adverse cardiac events, including arrhythmogenic right ventricular cardiomyopathy (ARVC), hypertrophic cardiomyopathy (HCM), myocarditis, and congenital coronary artery anomalies. Given the limitations of routine clinical examination and electrocardiographic (ECG) screening, echocardiography remains a cornerstone in the comprehensive assessment of cardiac structure and function. It provides detailed insights into the morphological and functional adaptations of both the LV and RV. Advanced echocardiographic modalities, such as speckle-tracking strain analysis and 3DE, enable more refined evaluation of myocardial deformation, offering essential tools to differentiate physiological adaptation from pathological remodeling.

Given these considerations, our findings highlight the importance of developing a well-applicable, reproducible, and preferably straightforward echocardiographic methodology for the early detection of potential maladaptive changes in this special population. By

refining the tools available to distinguish physiological from pathological remodeling in the young athlete's heart, we aim to improve risk stratification and thereby enhance the safety of sports participation. Our studies are designed to contribute toward advancing this goal.

2. OBJECTIVES

2.1. Quantifying the relative contributions of the longitudinal, radial, and anteroposterior motion components of global right ventricular function and examine their determining factors in a large cohort of healthy adult volunteers using 3D echocardiography

Global right ventricular function is governed by the interplay of multiple motion components that reflect the underlying myofiber architecture. However, the relative contribution of these components remains incompletely characterized. We hypothesize that shortening along the radial and anteroposterior axes holds comparable significance to longitudinal contraction in overall RV performance.

2.2. Quantifying the longitudinal, radial and anteroposterior components of global right ventricular function using 3D echocardiography in a cohort of healthy children and examine maturational changes in these parameters

Recently, 3DE has demonstrated excellent capability in quantifying RV volumes and has been validated against gold-standard imaging modalities in pediatric populations. Building on our initial study, we aimed to investigate the normal contraction patterns of the RV in healthy children.

2.3. The characterization of the right ventricular contraction pattern and its associations with exercise capacity in a large cohort of adolescent athletes using resting three-dimensional echocardiography

Pediatric athletes represent a unique population in which the interpretation of diagnostic findings poses significant clinical challenges; however, there remains a notable lack of data and evidence to guide this process (56, 57).

3. METHODS

3.1. Quantifying the relative contributions of the longitudinal, radial, and anteroposterior motion components of global right ventricular function and examine their determining factors in a large cohort of healthy adult volunteers using 3D echocardiography

Healthy volunteers of a wide age range were included from two centers (Semmelweis University, Budapest, Hungary, and the University of Occupational and Environmental Health, School of Medicine, Kitakyushu, Japan). Subjects were recruited from a community screening program, medical students, hospital employees, their relatives, and patients referred for cardiologic examination without known or subsequently established cardiovascular disease. The study protocol was approved by both centers' institutional ethical review boards (Semmelweis University: 169/2018; University of Occupational and Environmental Health: UOEHCRB18-015), and all participants gave written informed consent to participate in the study. To adequately assess the effects of ethnicity, age, and sex, both participating centers aimed to enroll ≥150 patients with an equal sex distribution across predefined age groups (30 men and 30 women per group). A total of 486 subjects (Hungary, n = 223; Japan, n = 263) were screened to achieve the desired sample size. Thirty-three patients were excluded because of the presence of exclusion criteria, and 3D RV analysis was not feasible in 15% of the subjects (n = 68). The final study population, with balanced age, sex, and ethnic distributions, was selected from this pool (n = 385). A routine physical examination, including anthropometric measurements, was performed in each subject, followed by blood pressure measurement and 12-lead ECG (electrocardiography). Body surface area (BSA) was calculated using the Mosteller formula (58). Inclusion criteria were age >20 years; no history and/or symptoms of any cardiovascular or pulmonary disease; and absence of cardiovascular risk factors such as arterial hypertension, diabetes, smoking, and dyslipidemia. Exclusion criteria were body mass index (BMI) ≥30 kg/m^2, any abnormality on ECG, moderate or severe valvular heart disease or wall motion abnormality and/or LV EF < 50% found during echocardiography, poor echocardiographic windows, and factors that might affect cardiac morphology and function, such as pregnancy and regular high-intensity sport activity (>3 h/wk) (59).

3.2. Quantifying the longitudinal, radial and anteroposterior components of global right ventricular function using 3D echocardiography in a cohort of healthy children and examine maturational changes in these parameters

Healthy children age <18 years were included from two centers: Boston Children's Hospital, Boston, MA, USA; and the Heart and Vascular Center of the Semmelweis University, Budapest, Hungary. Subjects at the Boston site were identified retrospectively from an existing database of 3DE images with accompanying clinical and demographic information. Patients in this database had presented to the outpatient clinic between 2014 and 2020 for evaluation of a common cardiac condition (most frequently murmur, chest pain, syncope, or family history of cardiac condition), were judged to have a structurally and functionally normal heart and were discharged from further follow-up. Exclusion criteria included structural abnormalities other than patent foramen ovale or trivial branch pulmonary stenosis (maximum instantaneous gradient < 15 mmHg within the first two years of life); arrhythmia (other than rare atrial or ventricular premature beats) including sinus bradycardia or tachycardia (heart rate z-score < −2 or > + 2 for age), acquired heart disease (cardiomyopathy, chemotherapy exposure, and Kawasaki disease), or co-morbidities with a potential impact on ventricular size and function (i.e., hypertension, renal failure, anemia, history of prematurity, chronic lung disease, pulmonary hypertension, obstructive sleep apnea, and connective tissue disorder). Healthy volunteers at the Semmelweis site were recruited from local schools; no individuals were identified subsequently with significant cardiac abnormalities revealed by echocardiography, ECG, blood pressure measurement, or review of medical history. Study protocols were approved by both centers' institutional review boards. Given the retrospective nature of recruitment at Boston Children's Hospital, informed consent was waived at that site. At Semmelweis University, families of all participants provided written informed consent to participate in the study. Blood pressure, height, and weight were recorded for all subjects (59). BSA was calculated using the Mosteller formula.

3.3. The characterization of the right ventricular contraction pattern and its associations with exercise capacity in a large cohort of adolescent athletes using resting three-dimensional echocardiography

Healthy, competitive, adolescent athletes were identified (n = 215) from our center's complex sports cardiology screening programme to be included in a retrospective, cross-sectional study. We defined the adolescents as over the age of 10 and under the age of 18 years. As an inclusion criterion, all athletes should have 3D transthoracic echocardiographic images available. A detailed medical history and training regime were obtained along with a standard physical examination and a 12-lead ECG. 2D and 3D echocardiography and then cardiopulmonary exercise testing (CPET) were performed on all athletes on the same day (time difference range between investigations: 0 to 3 hours). An age- and sex-matched healthy, sedentary population (n = 38) (no previous participation in intensive training, <3 h of exercise/week) served as the control group. These individuals also underwent the screening protocol except for CPET. This control group was recruited from local schools on a voluntary basis; no individuals were identified subsequently with significant cardiac abnormalities revealed by echocardiography, ECG, blood pressure measurement, or review of medical history. All participants and/or their legal family representative provided written, informed consent to the study procedures (59). BSA (to index volumetric measures with) was calculated using the Mosteller formula. This study is in accordance with the Declaration of Helsinki and approved by the local ethics committee.

3.4. Two-Dimensional Echocardiography

Echocardiographic acquisitions were performed using Philips EPIQ 7 (equipped with an X5-1 transducer; Philips Medical Systems, Best, the Netherlands) and GE Vivid E95 (equipped with 4V-D or 4Vc-D transducers; GE Healthcare, Horten, Norway) ultrasound systems. A standard acquisition protocol consisting of loops from parasternal, apical, and subxiphoid views was used according to current guidelines (42). LV internal diameters, wall thicknesses, and relative wall thickness; left atrial 2D end-systolic volume index (LAVi); mitral inflow velocities such as early (E) and late diastolic (A) peak velocities, their ratio, and E-wave deceleration time; systolic (s′), early diastolic (e′), and atrial (a′) velocities of the mitral lateral and septal annulus; average E/e′; RV basal short-axis diameter, TAPSE, FAC, right ventricular systolic pressure (RVSP), and right atrial 2D end-systolic volume index (RAVi) were measured according to current adult guidelines(40)·(25), and in accordance with the ASE standards for performing a pediatric

echocardiogram, LV volumes were calculated from the 5/6 × area × length formula and presented in raw fashion, as well as being indexed to BSA (60).

3.5. Three-Dimensional Echocardiography

Beyond the routine echocardiographic protocol, electrocardiographically gated full-volume 3D data sets reconstructed from four or six cardiac cycles optimized for the right or left ventricle were obtained for offline analysis. Image quality was verified at the bedside to avoid ‘‘stitching’’ and ‘‘dropout’’ artifacts of the 3D data. Further measurements were performed on a separate workstation using dedicated software (4D RV-Function 2 and 4D LV-Analysis 3; TomTec Imaging, Unterschleissheim, Germany). The algorithm detects the endocardial surface of the right and left ventricles, and following manual correction, it traces its motion throughout the cardiac cycle. We determined EDVi (end-diastolic volume index), ESVi (end-systolic volume index), and stroke volume index (SVi) normalized to BSA, and to characterize global RV and LV functions, EFs were also assessed. We measured LV mass index normalized to BSA by tracing the end-diastolic epicardial contour. Moreover, LV GLS and global circumferential strain (GCS) and 2D RV free wall longitudinal strain (FWLS) were also calculated.

3.6. Advanced three-dimensional echocardiographic analysis of the right ventricle

In order to quantify the three major functional components contributing to the global RV performance, we used the ReVISION software (Argus Cognitive, Inc, Lebanon, NH, USA). First, the 3D mesh model exported from the 4D RV-Function software package was re-oriented by a standard, automated method to identify the longitudinal (from the tricuspid annulus to the apex), radial (perpendicular to the interventricular septum), and anteroposterior (parallel to the interventricular septum) axes (Figure 1). Then, motion decomposition was performed along these directions in a vertex-based manner to quantify component values generated by each motion component [i.e., longitudinal EF (LEF), radial EF (REF), and anteroposterior EF (AEF)], as previously described (41). The relative contribution of each component to the total RV pump function was expressed as the ratio between LEF, REF, and AEF and total RVEF (LEF/RVEF, REF/RVEF, and AEF/RVEF, respectively). Notably, the absolute volume change of the RV is generated

by the aggregated contribution of the three motion components. This composition is not additive, rather multiplicative, and therefore, the sum of the decomposed volume changes is not equal to the global volume change. Thus, the relative contribution of the motion components (i.e., LEF/RVEF, REF/RVEF, AEF/RVEF) do not add up to 100%. To facilitate a better explainability, we also expressed the relative contributions as a signed parameter (i.e., LEF', REF', AEF'), where, for example, LEF'=LEF*[RVEF/(LEF+REF+AEF)], etc. With this method, the sum of the signed values adds up to the global RVEF (LEF'+REF'+AEF'=RVEF). Good reproducibility was previously reported by our laboratory concerning these metrics (41, 61).

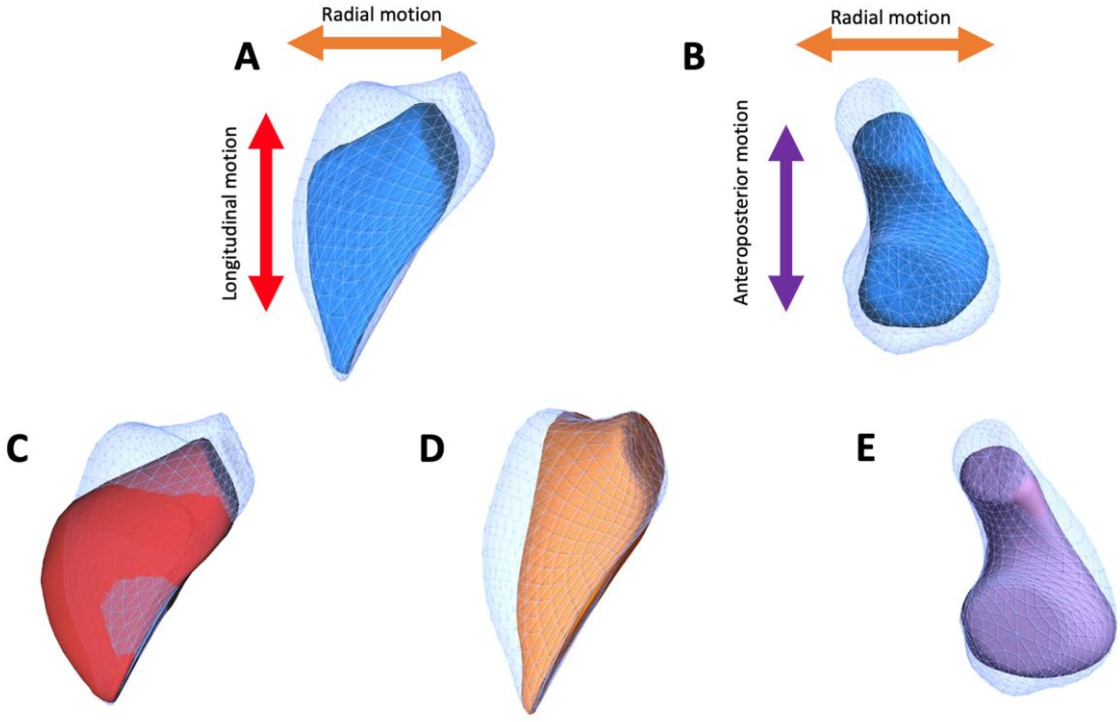

Figure 1. The three different components of right ventricular contraction from a representative subject (62). In the figure the global motion of the RV is shown from anterior (A) and superior (B) views (blue mesh, RV end-diastolic volume; blue surface, RV end-systolic volume). RV end-systolic meshes can be generated by "locking" the RV motion in two directions, permitting motion in only a single axis and thus revealing the impact of decomposed contraction components. Thus, the change in ventricular volume attributable to shortening along the longitudinal (C, red surface), radial (D, orange surface) and anteroposterior (E, purple surface) can be separately quantified.

3.7.1. Statistical analysis for quantifying the relative contributions of the longitudinal, radial, and anteroposterior motion components of global right ventricular function in a large cohort of healthy volunteers from two centers using 3D echocardiography

Data are presented as mean ± standard deviation (SD). The normal distribution of our variables was confirmed using a Shapiro-Wilk test. Unpaired Student's t tests were used to compare groups, and Pearson tests were performed for correlation analysis. In the case of 3D RV parameters, two-way analysis of variance (ANOVA) was used with two factors (age and sex), and their interactions were assessed to compare age groups. Repeated-measures ANOVA was used to compare the relative contributions in the pooled population and across age categories as well. Multiple linear regression analysis was applied to find independent predictors that determine RV motion components. To avoid multicollinearity issues, tolerance was set at >0.5. P values <0.05 were considered to indicate statistical significance (63).

3.7.2. Statistical analysis for describing the relative contributions of longitudinal, radial, and anteroposterior motion components of global right ventricular function in a cohort of healthy children

Continuous data were presented as mean ± SD or median and interquartile range. Categorical data were presented as counts and percentages (% of total population). Outcomes were summarized according to age groups representing different categories of patient body size: Infants: <1 year, Toddlers >1–5 years, School-Aged: >5–10 years, (Pre)Teens > 10–18 years. One-way ANOVA or the Kruskal Wallis H test was performed to compare the distribution of parameters by age group as appropriate. Wilcoxon signed-rank test was used to assess for differences in the contribution of LEF, REF, and AEF within each pre-specified age group, with Bonferroni correction applied (i.e., level of statistical significance set at $p < 0.017$). In order to assess the impact of patient sex on the EF parameters, a general linear model was used to compare EF means by sex with adjustment for age to produce least-squares means (59, 64). Data analyses were performed with SAS software (version 9.4, SAS Institute Inc., Cary, North Carolina) and R 4.1.2 (2021 The R Foundation for Statistical Computing Platform). P values <0.05 were used to indicate statistical significance.

3.7.3. Statistical analysis for the characterization of the right ventricular contraction pattern and its associations with exercise capacity in a large cohort of adolescent athletes

Using a previous study of similar methodology with smaller but more balanced sample sizes (60 athletes vs. 40 controls)(65), we determined the effect-sizes (Cohen's d) of representative parameters that describe left- and right ventricular morphology and function (LV EDVi, LV EF, RV EDVi, RV EF, LEF/RVEF). After calculating Cohen's d, all of these parameters were considered to have a relatively large/medium effect size (Cohen's d values respectively: 2.616, 1.527, 2.418, 1.193, 1.175). Using these calculated effect sizes, we performed power analysis on the retrospectively identified participants from our database. In all cases, the statistical power exceeded 0.80, reassuring that the outlined sample size that we proposed for our current study was appropriate despite its unbalanced nature. Statistical analysis was performed using dedicated software (StatSoft Statistica, v12, Tulsa, OK, USA). Continuous variables are presented as mean ± SD, whereas categorical variables are reported as frequencies and percentages. After verifying the normal distribution of each variable using the Kolmogorov-Smirnov test, groups were compared with the unpaired Student's t test or Mann–Whitney U test for continuous variables and the $\chi 2$ or Fisher's exact test for categorical variables, as appropriate. The Pearson or Spearman test was computed to assess the correlation between continuous variables. A two-sided P-value of <0.05 was considered statistically significant.

3.8. Cardiopulmonary exercise testing

CPET for VO_2 and peak oxygen uptake indexed to body weight (VO_2/kg) quantification was performed on a treadmill on institutional, sport-specific, incremental protocols (starting with a 1-min sitting resting phase, followed by 1–2 min flat walk of 6 km/h as warm-up, then by continuous 8–10 km/h uphill running with an increasing slope of 1.0–1.5% every minute until exhaustion) (66). The volume and composition of the expired gases were analyzed breath by breath using an automated cardiopulmonary exercise system (Respiratory Ergostik, Geratherm, Bad Kissingen, Germany). Participants were encouraged to achieve maximal effort. Maximal intensity was considered to be achieved, if the athlete reported maximal subjective exhaustion and either the respiratory exchange

ratio (RER) was over 1.1, and/or flattening could be seen in the oxygen uptake and the heart rate (HR) curves.

4. RESULTS

4.1. Quantifying the relative contributions of the longitudinal, radial, and anteroposterior motion components of global right ventricular function and investigating their determining factors in a large cohort of healthy volunteers from two centers using 3D echocardiography

4.1.1. Morphometric and conventional echocardiographic characteristics

The mean age of the enrolled patients was 45±16 years. Men were characterized by significantly higher morphometric parameters, higher systolic and DBP (diastolic blood pressure), and lower HR (Table 1). Male sex was associated with higher RV basal diameter, RV areas, right atrial volume index (RAVi), and LV volumes and LV mass index. RV FAC and RV FWLS were higher in women, but TAPSE did not differ between sexes (59, 64). Doppler tissue imaging–derived tricuspid annular velocities and pulmonary artery systolic pressure (PASP) were comparable between men and women (Table 2).

Table 1. Clinical and demographic characteristics of the study group

	All (N=300)	Female (n=150)	Male (n=150)	P
Age, y	44.8 ± 15.6	44.9 ± 15.6	44.7 ± 15.6	0.87
Height, cm	167.2 ± 10.1	160.6 ± 7.6	173.9 ± 7.6	<0.001
Weight, kg	66.7 ± 14.6	59.1 ± 12.1	74.3 ± 12.8	<0.001
BMI, kg/m^2	23.7 ± 3.9	22.8 ± 4.0	24.5 ± 3.6	<0.001
BSA, m^2	1.75 ± 0.23	1.62 ± 0.19	1.89 ± 0.19	<0.001
SBP, mm Hg	131.6 ± 15.4	128.3 ± 15.4	135.2 ± 14.8	<0.001
DBP, mm Hg	76.7 ± 11.2	75.3 ± 12.0	78.2 ± 10.1	<0.05
HR, beats/min	68.8 ± 13.5	70.4 ± 14.5	67.0 ± 12.1	<0.05

BMI, Body mass index; BSA, body surface area; DBP, diastolic blood pressure; SBP, systolic blood pressure; HR, heart rate. Data are expressed as mean ± SD.

Table 2. Basic echocardiographic characteristics of the study group

	All (N=300)	Female (n=150)	Male (n=150)	P
RV basal diameter, mm	32.3 ± 5.9	30.2 ± 5.5	34.3 ± 5.0	<0.001

RVEDA, cm^2	24.6 ± 5.8	21.6 ± 4.6	27.7 ± 5.2	<0.001
RVESA, cm^2	15.0 ± 3.6	12.9 ± 2.7	17.2 ± 3.1	<0.001
RV FAC, %	50.2 ± 7.5	51.9 ± 7.6	48.5 ± 7.0	<0.001
TAPSE, mm	22.2 ± 4.8	21.9 ± 4.6	22.5 ± 5.0	0.31
Tricuspid annular s', cm/sec	13.8 ± 2.5	13.7 ± 2.5	13.9 ± 2.4	0.50
Tricuspid annular e', cm/sec	15.5 ± 4.2	15.7 ± 4.4	15.2 ± 4.0	0.46
Tricuspid annular a', cm/sec	15.2 ± 6.7	14.6 ± 4.6	15.8 ± 8.2	0.32
RV 2D FWLS, %	-29.9 ± 5.4	-30.8 ± 5.6	-29.1 ± 5.0	<0.01
PASP, mm Hg	25.3 ± 5.7	25.8 ± 5.3	24.8 ± 6.1	0.20
RAVi, mL/m^2	20.8 ± 9.8	19.2 ± 8.8	22.3 ± 10.5	<0.01
3D LVEDVi, mL/m^2	63.6 ± 12.8	60.0 ± 10.6	67.2 ± 13.7	<0.001
3D LVESVi, mL/m^2	27.0 ± 7.5	24.5 ± 5.9	29.6 ± 8.0	<0.001
3D LVEF, %	57.8 ± 6.1	59.1 ± 6.3	56.4 ± 5.6	<0.001
3D LV GLS, %	-20.0 ± 2.9	-21.2 ± 2.6	-18.9 ± 2.6	<0.001
3D LV GCS, %	-27.8 ± 4.4	-28.4 ± 4.4	-27.2 ± 4.2	<0.05
3D LV Mi, g/m^2	62.0 ± 11.0	59.4 ± 10.3	64.6 ± 11.0	<0.001

a', peak late (atrial) diastolic annular velocity; e', early diastolic annular velocity; EF, ejection fraction; FAC, fractional area change; FWLS, Free wall longitudinal strain; GCS, global circumferential strain; GLS, global longitudinal strain; LV, left ventricle; LVEDVi, LV end-diastolic volume index; LVESVi, LV end-systolic volume index; LV Mi, LV mass index; PASP, pulmonary artery systolic pressure; RAVi, right atrial end-systolic volume index; RV, right ventricle; RVEDA, RV end- diastolic area; RVESA, RV end-systolic area; s', systolic annular velocity; TAPSE, tricuspid annular plane systolic excursion; Data are expressed as mean ± SD.

4.1.2. Three-dimensional right ventricular mechanics of the study group by age categories and sex

Men had significantly higher RV end-diastolic volume index (RVEDVi) and RV end-systolic volume index, while RVEF, RV GLS, RV GCS, and RV global area strain (GAS) were significantly higher in women. Values of longitudinal EF index (LEFi), radial EF index (REFi), and anteroposterior EF index (AEFi) showed that there were no sex differences in the relative contributions of the longitudinal, radial, and anteroposterior motion components. RV volumetric indices, RVEF, RV GLS, RV GAS, and

circumferential EF index significantly differed across age categories. No significant interaction between age and gender was found regarding 3D RV parameters. The contribution of nonlongitudinal motion components measured by circumferential EF index was markedly higher in the pooled population and in every age category compared with longitudinal shortening ($P < 0.001$ for all). Circumferential shortening was further decomposed to radial and anteroposterior shortening. Anteroposterior (49.1±6.8%) and longitudinal shortening (46.6±8.7%) were found to be the most prominent motion components of the RV in the pooled population, while radial shortening (43.5±10.3%) was of inferior significance. When analyzing the age categories separately, the relative contribution of longitudinal shortening was significantly higher compared with the radial component in younger age categories (20–29 and 30–39 years). In the older groups, however, LEFi and REFi were comparable. Anteroposterior shortening had a higher contribution compared with longitudinal shortening in the 30 to 39 and 50 to 59 age groups, while it had a higher contribution compared with radial shortening in every age category except 50 to 59 years (Table 3, Figure 2). We compared subjects in the lowest quartile of LEFi with the rest of the study group (37.7±4.0% vs 48.9±5.2%, $P<0.001$). A lower contribution of longitudinal shortening was not associated with lower RVEF (59.5±6.3% vs 59.0±5.4%, $P =0.67$), and AEFi was also comparable between the two groups (50.4±6.7% vs 48.7±6.8%, $P =0.12$); however, the contribution of radial shortening was significantly higher (REFi 50.5±7.2% vs 41.0±10.0%, $P<0.001$). We also compared subjects in the lowest quartile of REFi with the rest of the population (29.7±7.4% vs 48.0±6.3%, $P <0.001$). Although patients with the lowest REFi had significantly lower RVEFs (55.4±6.2% vs 60.4±4.9%, $P <0.001$), LEFi (52.1±6.1% vs 43.8±6.2%, $P <0.001$) and AEFi (51.6±6.1% vs 48.3±6.8%, $P < 0.001$) were significantly higher, suggesting that the other two motion directions may effectively compensate lower radial shortening (59, 64).

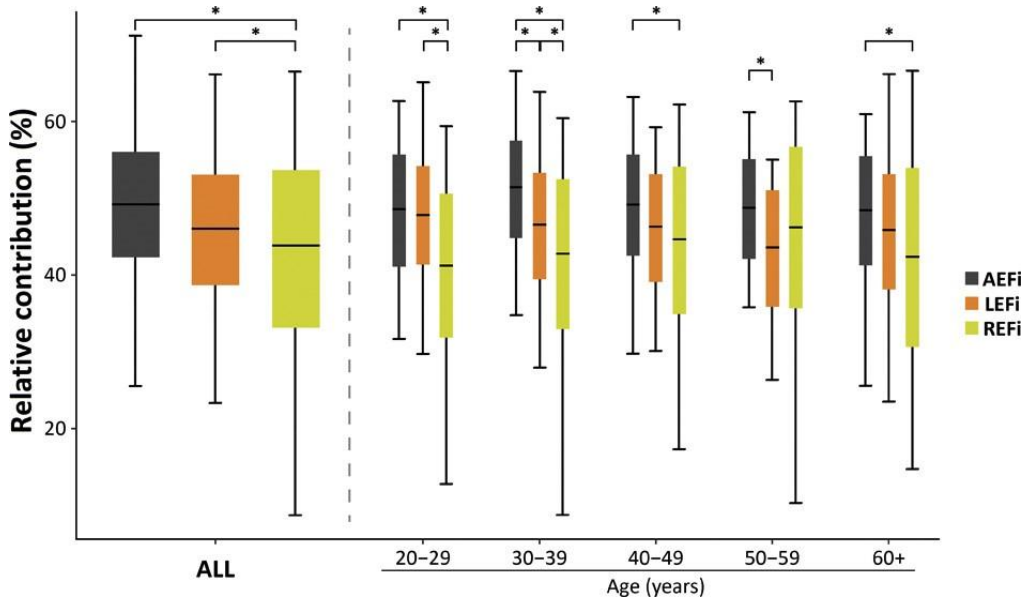

*Figure 2. Comparison of the relative contributions of anteroposterior, longitudinal, and radial shortening to global RV function (62). Individual and mean values of AEFi, LEFi, and REFi are visualized in the pooled population (n = 300) and the different age categories, with statistical comparison among the three motion components. *P <0.05. The bar charts present mean values with standard deviation, while the whiskers indicate the minimum and maximum values.*

Table 3. Three-dimensional RV mechanics of the study group by age categories and sex									
	All	**20-29 y**	**30-39 y**	**40-49 y**	**50-59 y**	**≥60 y**	**P value for age**	**P value for gender**	**Interaction P**
RVEDVi, mL/m2									
Men	57.0±12.3	62.7±12.4	58.76±14.0	53.1±10.2	54.0±10.2	56.3±12.4			0.72
Women	50.7±11.6	54.6±12.3	50.9±10.6	46.2±10.2	51.3±13.4	50.5±10.2			
All	53.8±12.3	58.6±12.9	54.8±12.9	49.7±10.7	52.7±11.8	53.4±11.7	<0.01	<0.001	
RVESVi, mL/m2									
Men	24.1±6.2	26.6±6.4	23.8±6.5	22.1±4.8	23.0±6.5	25.2±5.8			0.91
Women	19.8±5.3	21.4±5.5	19.4 ± 4.6	18.1 ± 5.1	20.2 ± 6.4	20.2±4.2			
All	22.0±6.1	24.0±6.4	21.6±6.0	20.1±5.3	21.6±6.6	22.7±5.6	<0.01	<0.001	
RVEF, %									
Men	57.3±5.4	57.6±4.8	59.5±4.5	58.4±5.1	56.0±6.0	55.1±5.8			0.69
Women	61.1±5.3	60.7±4.6	61.9±4.5	61.9±4.2	60.9±6.4	59.6±6.4			
All	59.2±5.7	59.1±4.9	60.7±4.6	60.1±5.0	58.5±6.6	57.3±6.5	<0.01	<0.001	

RV GLS, %									
Men	-29.2±5.5	-29.7±5.1	-31.9±4.7	-29.5±5.2	-27.3±5.6	-27.4±5.8			0.91
Women	-33.1±6.6	-33.6±4.6	-35.6±5.5	-33.4±5.7	-33.3±7.4	-30.4±8.3			
All	-31.1±6.4	-31.7±5.2	-33.7±5.4	-31.5±5.8	-29.8±7.0	-28.9±7.2	<0.001	<0.001	
RV GCS, %									
Men	-27.2±6.3	-26.9±6.5	-28.9±5.7	-28.1±7.1	-26.3±5.6	-25.5±6.2			0.48
Women	-29.9±7.9	-29.3±6.6	-29.9±8.1	-29.4±7.1	-31.5±9.4	-29.2±8.2			
All	-28.5±7.2	-28.1±6.6	-29.4±7.0	-28.8±7.1	-28.9±8.1	-27.4±7.4	<0.57	<0.01	
RV GAS, %									
Men	-38.2±4.9	-38.3±4.2	-39.6±4.6	-39.1±4.7	-37.4±5.4	-36.7±5.1			0.90
Women	-41.8±5.0	-41.7±3.8	-43.1±3.6	-41.7±4.1	-41.6±6.3	-40.8±6.5			
All	-40.0±5.2	-40.0±4.3	-41.4±4.5	-40.4±4.6	-39.5±6.2	-38.7±6.1	<0.05	<0.001	
LEFi, %									
Men	46.2±8.8	46.8±7.3	47.3±10.0	46.9±8.4	44.0±10.8	45.8±7.4			0.92
Women	46.9±8.6	47.0±7.5	49.0±9.5	48.7±8.3	44.9±7.5	45.1±9.7			
All	46.6±8.7	46.9±7.3	48.2±9.7	47.8±8.3	44.5±9.3	45.3±8.5	0.10	0.43	
CEFi, %									
Men	79.0±6.6	77.1±6.3	80.3±5.8	79.8±6.1	80.4±7.3	77.5±7.4			0.88

Women	78.8±7.0	76.6±7.7	78.9±6.9	79.4±5.2	80.9±6.6	78.4±8.0			
All	78.9±6.8	76.8±6.8	79.6±6.3	79.6±5.6	80.7±6.9	77.9±7.7	0.02	0.80	
REFi, %									
Men	43.6±9.4	41.7±8.9	42.5±7.0	44.7±10.1	46.4±9.4	42.7±11.0			0.99
Women	43.2±11.1	40.7±9.9	42.9±12.0	44.4±9.3	46.0±11.6	41.8±12.4			
All	43.5±10.3	41.2±9.4	42.7±9.7	44.5±9.6	46.2±10.5	41.8±12.4	0.07	0.72	
AEFi, %									
Men	48.5±6.4	47.6±7.3	51.8±6.9	48.7±5.6	47.5±5.3	47.0±6.0			0.50
Women	49.7±7.1	49.2±7.3	50.5 ± 5.7	49.5 ± 7.5	49.7 ± 7.4	49.8±7.9			
All	49.1±6.8	48.4±7.3	51.2±6.3	49.16±6.6	48.6±6.5	48.4±7.1	0.13	0.12	

AEFi, anteroposterior EF index; CEFi: circumferential ejection fraction index; EF, ejection fraction; GAS, global area strain; GCS, global circumferential strain; GLS, global longitudinal stain; LEFi, longitudinal EF index; REFi, radial EF index; RV, right ventricle; RVEDVi, RV end-diastolic volume index; RVESVi, RV end-systolic volume index. Data are expressed as mean ± SD.

4.1.3. Correlations of right ventricular parameters and basic morphometric and demographic parameters

Several RV parameters showed weak but statistically significant correlations with age, BSA, and hemodynamic parameters (Table 4). Age correlated negatively with RVEDVi, RVEF and LEFi, while it showed a positive correlation with RV GLS and RV GAS. BSA showed negative relationships with RVEF, LEFi, and AEFi but correlated positively with RVEDVi, REFi and RV GLS. Regarding SBP and DBP, negative correlations were found with AEFi, while RVEDVi, REFi and RV GLS had positive correlations with blood pressure. Systolic blood pressure (SBP) also correlated negatively with RVEF. HR showed positive relationships with RVEF and REFi but correlated negatively with RV GCS, RV GAS and AEFi. PASP did not show any correlation with RV parameters in the pooled study group (Table 4). In subjects ≥60 years of age, however, RVEF ($r = 0.45$, $P < 0.05$) and REFi ($r = 0.49$, $P < 0.01$) showed weak negative correlations with PASP (59, 64).

Table 4. Univariate correlations between RV parameters and basic morphometric and demographic parameters						
	Age	**BSA**	**PASP**	**SBP**	**DBP**	**HR**
RVEDVi	**r = -0.14**	**r = 0.37**	r = 0.01	**r = 0.18**	**r = 0.15**	r = -0.11
	P = 0.02	**P < 0.001**	P = 0.90	**P < 0.01**	**P = 0.02**	P = 0.07
RVEF	**r = -0.18**	**r = -0.18**	r = -0.09	**r = -0.14**	r = -0.05	**r = 0.17**
	P <0.01	**P < 0.01**	P = 0.20	**P = 0.03**	P = 0.42	**P < 0.01**
RV GLS	**r = 0.23**	**r = 0.26**	r = 0.08	**r = 0.17**	**r = 0.13**	r = -0.001
	P <0.001	**P < 0.001**	P = 0.28	**P < 0.01**	**P = 0.04**	P = 0.95
RV GCS	r = 0.07	r = 0.05	r = 0.02	r = 0.09	r = 0.03	**r = -0.14**
	P = 0.25	P = 0.46	P = 0.80	P = 0.18	P = 0.59	**P = 0.03**
RV GAS	**r = 0.16**	**r = 0.13**	r = 0.08	r = 0.10	r = 0.04	**r = -0.19**
	P <0.01	**P = 0.02**	P = 0.24	P = 0.11	P = 0.51	**P < 0.01**
LEFi	**r = -0.11**	**r = -0.18**	r = -0.13	r = -0.12	r = -0.11	r = -0.11
	P = 0.048	**P < 0.01**	P = 0.07	P = 0.06	P = 0.09	P = 0.08
REFi	r = 0.06	**r = 0.20**	r = -0.02	**r = 0.15**	**r = 0.24**	**r = 0.23**
	P = 0.28	**P < 0.001**	P = 0.79	**P = 0.02**	**P < 0.001**	**P <0.001**
AEFi	r = -0.07	**r = -0.21**	r = 0.07	**r = -0.21**	**r = -0.25**	**r = -0.15**
	P = 0.24	**P < 0.001**	P = 0.33	**P < 0.01**	**P < 0.001**	**P = 0.02**

AEFi, anteroposterior EF index; DBP, Diastolic blood pressure; EF, ejection fraction; GAS, global area strain; GCS, global circumferential strain; GLS, global longitudinal strain; LEFi, longitudinal EF index; REFi, radial EF index; RV, right ventricle; RVEDVi, RV end-diastolic volume index; SBP, systolic blood pressure. Values in boldface type are statistically significant (P < 0.05).

4.1.4. Independent predictors of LEFi, REFi and AEFi

Multivariate models were built with relevant hemodynamic and echocardiographic variables to find independent predictors of LEFi, REFi, and AEFi (Table 5, 6 and 7). Age, BSA, HR, and RVEDVi were independent predictors of LEFi and REFi as well, but all with the opposite effect on the two motion directions. Beyond these variables, LV mass index, LV GLS, and PASP were associated with LEFi in the multivariate analysis. Concerning REFi, RVEF and LVEF were found to be independent predictors. Race, LVEF, and RVEF were independent predictors of AEFi (Table 7).

Table 5. Multivariate linear regression analysis: independent predictors of LEFi

Covariate	β	P
Age	**-0.23**	**<0.01**
Sex	-0.13	0.29
Race	-0.03	0.29
BSA	**-0.29**	**<0.001**
SBP	0.15	0.7
DBP	0.05	0.57
HR	**-0.17**	**<0.05**
LVEDVi	-0.01	0.88
LVEF	-0.17	0.60
LV Mi	**0.21**	**<0.05**
LV GLS	**-0.16**	**<0.05**
LV GCS	-0.23	0.42
PASP	**-0.15**	**<0.05**
RVEDVi	**-0.20**	**<0.05**
RVEF	-0.15	0.07
Adjusted R^2	0.15	
SE	6.41%	
Cumulative P value	<0.0001	

BSA, body surface area; DBP, Diastolic blood pressure; EF, ejection fraction; GCS, global circumferential strain; GLS, global longitudinal strain; HR, heart rate; LEFi, longitudinal EF index; LV, left ventricle; LVEDVi, LV end-diastolic volume index; LV

Mi, LV mass index; PASP, pulmonary artery systolic pressure; RV, right ventricle; RVEDVi, RV end-diastolic volume index; SBP, systolic blood pressure. Values in boldface type are statistically significant (P < .05).

Table 6. Multivariate linear regression analysis: independent predictors of REFi		
Covariate	**β**	**P**
Age	**0.24**	**<0.001**
Sex	0.05	0.68
Race	0.009	0.94
BSA	**0.29**	**<0.001**
SBP	-0.13	0.16
DBP	0.10	0.23
HR	**0.21**	**<0.01**
LVEDVi	-0.02	0.86
LVEF	**-0.22**	**<0.01**
LV Mi	-0.10	0.19
LV GLS	-0.03	0.83
LV GCS	0.04	0.86
PASP	0.001	0.99
RVEDVi	**0.22**	**<0.01**
RVEF	**0.56**	**<0.001**
Adjusted R^2	0.32	
SE	8.39%	
Cumulative P value	<0.0001	

BSA, body surface area; DBP, Diastolic blood pressure; EF, ejection fraction; GCS, global circumferential strain; GLS, global longitudinal strain; HR, heart rate; LV, left ventricle; LVEDVi, LV end-diastolic volume index; LV Mi, LV mass index; PASP, pulmonary artery systolic pressure; REFi, radial EF index; RV, right ventricle; RVEDVi, RV end-diastolic volume index; SBP, systolic blood pressure. Values in boldface type are statistically significant (P < .05).

Table 7. Multivariate linear regression analysis: independent predictors of AEFi		
Covariate	**β**	**P**
Age	-0.005	0.95
Sex	0.005	0.96
Race	**0.25**	**<0.05**
BSA	0.01	0.92
SBP	-0.03	0.79
DBP	-0.04	0.66
HR	-0.06	0.47
LVEDVi	0.15	0.08
LVEF	**0.44**	**<0.05**
LV Mi	-0.08	0.50
LV GLS	0.09	0.48
LV GCS	0.25	0.26
PASP	0.09	0.25
RVEDVi	-0.17	0.05
RVEF	**0.26**	**<0.01**
Adjusted R^2	0.20	
SE	6.41%	
Cumulative P value	<0.0001	

AEFi, anteroposterior EF index; BSA, body surface area; DBP, Diastolic blood pressure; EF, ejection fraction; GCS, global circumferential strain; GLS, global longitudinal strain; HR, heart rate; LV, left ventricle; LVEDVi, LV end-diastolic volume index; LV Mi, LV mass index; PASP, pulmonary artery systolic pressure; RVEDVi, RV end-diastolic volume index; SBP, systolic blood pressure. Values in boldface type are statistically significant (P < .05).

4.1.5. Presentation the importance of detailed analysis of right ventricular deformation

We have included three representative cases, all with maintained RVEFs, to highlight the importance of a detailed analysis of RV deformation pattern (Figure 3).

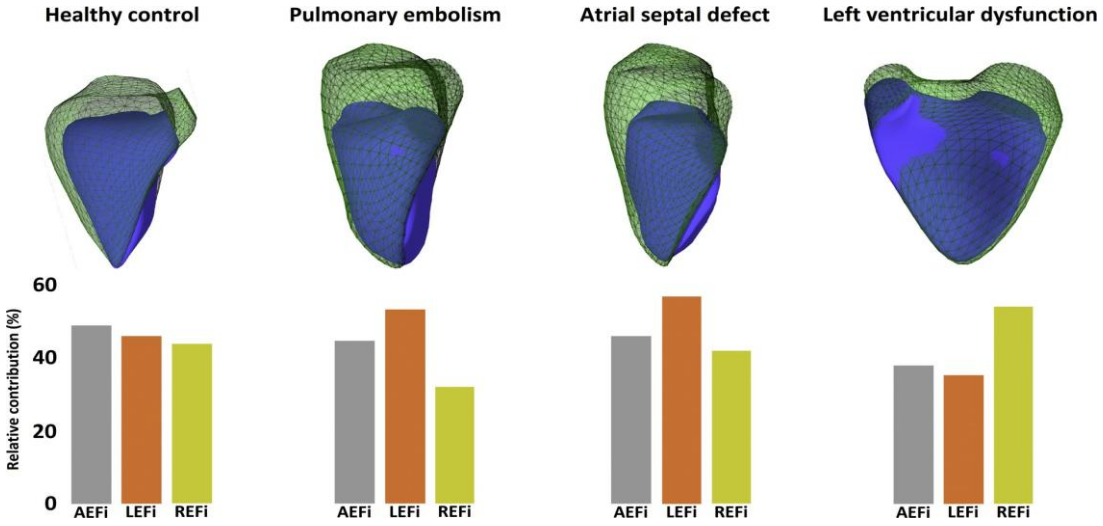

Figure 3. Significant changes in RV deformation pattern with maintained RVEF: representative cases (62). A healthy subject from our study group (RVEF 62%) demonstrates physiologic RV deformation with more or less equal contribution of the three motion directions. In a patient following massive pulmonary embolism (pressure overload; PASP 57 mm Hg) and maintained global RV function (RVEF 51%), radial motion (REFi) was significantly lower, while anteroposterior shortening (AEFi) remained unchanged, resulting in a higher contribution of longitudinal motion to global function (LEFi). A patient with a hemodynamically significant atrial septal defect (volume overload; Qp/Qs = 1.8) was characterized by hyperdynamic RV function (RVEF 66%). In this case, higher LEFi could be seen, with subsequently lower REFi and AEFi. In a patient with HF with nonischemic dilated cardiomyopathy, severely reduced LV function (LVEF 29%), and maintained RV systolic function (RVEF 48%), LEFi and AEFi were severely reduced, while REFi was relatively increased.

4.2. Describing the relative contributions of longitudinal, radial, and anteroposterior motion components of global right ventricular function in a cohort of healthy children and examining differences in the relative contributions of the 3 components of ejection fraction in children and looking for changes in the contribution of these components as a function of age

4.2.1. Morphometric and demographic characteristics

The study population included 166 subjects (Boston = 76; Semmelweis = 90). The median age of subjects was 13.8 years (IQR 8.6 to 15.3), with a skewed distribution towards the oldest age group (as a consequence of the recruitment strategy at the Semmelweis site). The population was majority male (n = 131, 79%), driven by a male-predominant population recruited at the Semmelweis site (n = 81, 90%) (Table 8).

Table 8. Patient characteristics

	All (n = 166)	Infants (n = 13)	Toddlers (n = 11)	School-Aged (n = 21)	(Pre)Teens (n = 121)	P-value
Age, year	13.8 (8.6, 15.3)	0.1 (0.05, 0.1)	3.6 (3.3, 4.1)	6.3 (5.2, 7.9)	14.4 (13.6, 15.7)	<0.001
Female (n(%))	35 (21%)	7 (54%)	5 (45%)	7 (33%)	16 (13%)	
Height, m	1.49±0.38	0.53±0.07	1.00±0.08	1.21±0.11	1.69±0.14	<0.001
Weight, kg	47.7±23.8	4.2±2.0	16.6±3.2	23.3±5.9	59.4±15.3	<0.001
BMI, kg/m^2	19.1±3.5	14.3±2.0	16.3±1.4	15.5±1.5	20.5±3.0	<0.001
BSA, m^2	1.39±0.54	0.25±0.07	0.68±0.09	0.88±0.14	1.66±0.29	<0.001
SBP, mmHg	117±19	92±14	100±10	100±10	125±16	<0.001
DBP, mmHg	65±12	53±11	53±6	56±8	68±10	<0.001
HR, beats/min	80±20	130±13	89±12	84±14	73±12	

Continuous data are expressed as mean ±SD, with the exception of age which are presented as median (IQR). BMI, body mass index; BSA, body surface area; DBP, diastolic blood pressure; HR, heart rate; SBP, systolic blood pressure.

4.2.2. Conventional echocardiographic parameters

TAPSE increased significantly with age. Most subjects had either no (92, 53%) or trivial (72, 42%) tricuspid regurgitation. There were no differences between groups in terms of RV FAC. Age-related variation in 2D FWLS was present, with the largest absolute values seen in the toddler and school-aged groups (Table 9).

Table 9. Conventional echocardiographic characteristics						
	All (n = 166)	**Infants (n = 13)**	**Toddlers (n = 11)**	**School-Aged (n = 21)**	**(Pre)Teens (n = 121)**	**P-value**
TAPSE, mm	21.8 (16.9, 26.1)	6.2 (4.5, 9.0)	14.3 (12.0, 19.7)	17.1 (15.3, 19.6)	23.7 (20.9, 27.8)	<0.001
RV FAC, %	48.8 (45.3, 52.4)	46.5 (42.9, 51.2)	51.3 (44.7, 54.2)	50.7 (48.7, 54.2)	48.5 (45.3, 52.2)	0.161
RV 2D FWLS, %	-30.4 (-33.7, -26.2)	−29.8 (−31.8, −23.2)	-34.8 (-39.0, -28.4)	-32.1 (-36.6, -30.9)	-29.4 (-33.0, -26.2)	0.016
2D LVEDV, ml	113.9 (74.6, 145.6)	9.4 (7.7, 11.1)	48.6 (39.0, 55.9)	62.8 (55.7, 74.6)	135.0 (110.9, 154.6)	<0.001
2D LVEDVi, ml/m^2	77.2 (67.1, 85.8)	42.7 (35.0, 43.5)	70.8 (60.9, 75.5)	70.4 (66.8, 79.3)	79.8 (73.0, 88.9)	<0.001
2D LVESV, ml	45.2 (26.3, 60.9)	3.7 (3.0, 3.9)	17.3 (12.5, 18.2)	21.3 (20.1, 26.3)	54.8 (42.5, 66.1)	<0.001
2D LVESVi, ml/m^2	30.1 (24.9, 35.4)	14.6 (12.7, 16.5)	23.4 (21.1, 25.8)	25.3 (23.4, 26.8)	32.7 (28.1, 36.7)	<0.001
LV EF, %	60.4 (57.0, 63.9)	61.5 (59.0, 64.3)	65.9 (64.0, 67.9)	64.0 (62.6, 67.0)	58.9 (56.3, 62.0)	<0.001

Data are expressed as median (Q1, Q3). 2D, two-dimensional; EDV, end-diastolic volume; EF, ejection fraction; ESV, end-systolic volume; FAC, fractional area change; FWLS, free wall longitudinal strain; LV, left ventricle; LVEDVi, indexed left ventricular end-diastolic volume; LVESVi, indexed left ventricular end-systolic volume; RV, right ventricle; TAPSE, tricuspid annulus plane systolic excursion.

4.2.3. Three-dimensional echocardiographic analysis of right ventricular size and ejection fraction components

RV volumes, global RVEF, REF, REFi, and longitudinal as well as circumferential 3D strain parameters showed significant age-related differences. Additionally, age-related differences were seen for all components of RV strain (Table 10). No differences were identified between male and female subgroups in regards of sex-specific age-adjusted mean values for the EF parameters. Figure 4 shows the EF components for the entire cohort as well as broken down by age group. For the entire cohort, the AEF was greater than the other two components. A similar pattern was observed across all age groups, although statistical significance was reached only in the oldest cohort. No significant differences were observed among any components in the infants and toddlers (59, 64).

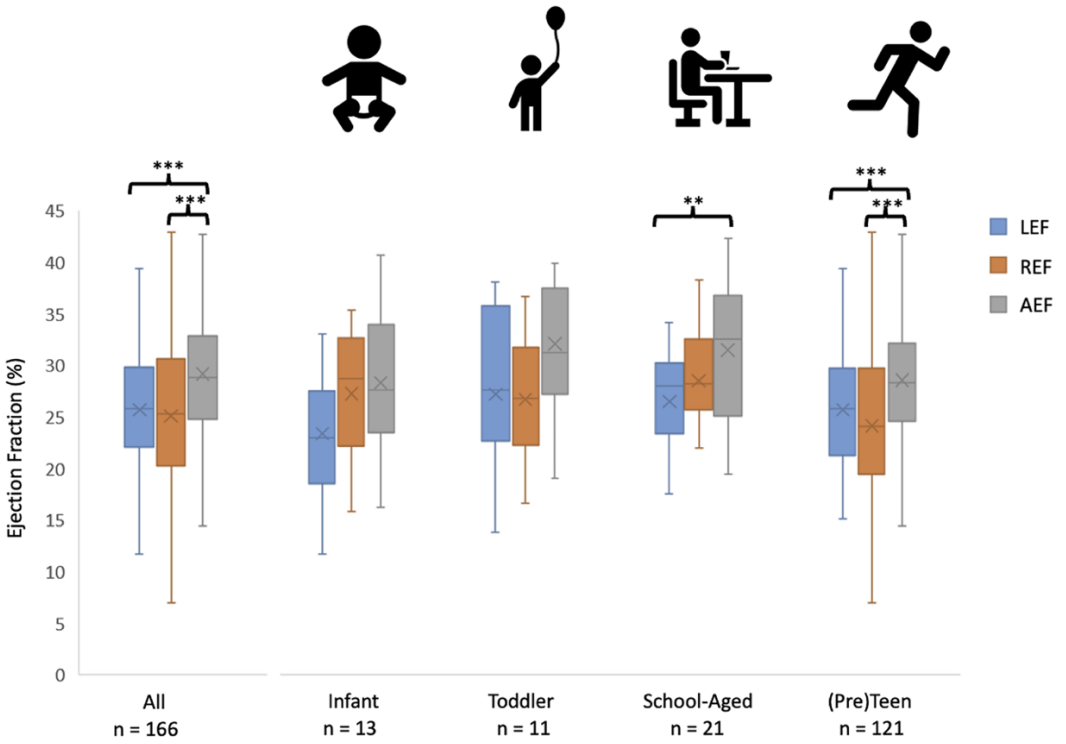

*Figure 4. A comparison of the contributions of longitudinal, radial and anteroposterior EF components to global RV function (67). **p < 0.01, ***p < 0.001. Boxplots show the interquartile range (Q1–Q3); the central line indicates the median, × denotes the mean, and whiskers represent the minimum and maximum values.*

Table 10. Three-dimensional echocardiographic analysis of right ventricular size and ejection fraction components						
	All (n = 166)	**Infants (n = 13)**	**Toddlers (n = 11)**	**School-aged (n = 21)**	**(Pre)Teens (n = 121)**	**P-value**
3D RVEDV, ml	115.3 (66.0, 149.6)	9.4 (8.0, 10.0)	43.5 (37.5, 47.7)	56.3 (52.4, 64.3)	133.4 (107.2, 157.0)	**<0.001**
3D RVEDVi, ml/m^2	74.8 (64.4, 87.3)	40.7 (38.0, 43.1)	64.4 (59.4, 67.9)	66.4 (59.9, 73.8)	80.1 (71.0, 89.9)	**<0.001**
3D RVESV, ml	47.1 (25.6, 63.3)	3.9 (3.3, 4.9)	16.4 (15.2, 19.5)	22.4 (18.4, 25.6)	56.8 (43.0, 70.3)	**<0.001**
3D RVESVi, ml/m^2	31.6 (24.6, 37.4)	16.0 (14.9, 18.8)	24.6 (22.2, 28.1)	25.8 (23.4, 27.4)	33.8 (28.8, 39.4)	**<0.001**
RV EF, %	58.1 (54.6, 61.4)	55.1 (52.7, 61.1)	59.3 (55.0, 65.0)	62.1 (58.4, 64.6)	57.3 (54.3, 61.0)	**0.008**
LEF, %	25.8 (22.1, 29.8)	23.0 (19.3, 27.2)	27.6 (22.7, 35.8)	28.0 (23.4, 29.8)	25.8 (21.3, 29.7)	0.345
REF, %	25.3 (20.3, 30.6)	28.7 (22.6, 32.2)	26.8 (22.3, 31.7)	28.2 (25.7, 32.2)	24.1 (19.5, 29.7)	**0.020**
AEF, %	28.8 (24.8, 32.9)	27.6 (24.1, 33.8)	31.2 (27.2, 37.5)	32.6 (25.1, 36.4)	28.3 (24.7, 32.2)	0.109
LEFi, %	43.8 (39.1, 50.2)	43.0 (33.7, 43.7)	43.7 (40.8, 57.5)	43.7 (42.1, 51.1)	44.9 (38.2, 49.9)	0.436
REFi, %	43.7 (35.3, 51.3)	48.2 (42.8, 53.6)	45.8 (33.8, 59.2)	48.0 (43.4, 50.8)	42.4 (34.0, 51.1)	0.055
AEFi, %	50.7 (43.1, 55.6)	52.2 (41.5, 54.4)	57.2 (46.6, 60.9)	53.0 (42.1, 58.2)	50.5 (43.5, 54.0)	0.353
3D GAS, %	−40.3 (−43.7, −37.3)	−37.6 (−43.8, −34.4)	−43.8 (−44.8, −37.7)	−43.1 (−45.0, −39.0)	−40.1 (−42.7, −37.0)	**0.046**
3D GLS, %	−22.9 (−25.8, −20.5)	−18.9 (−23.7, −17.5)	−25.9 (−26.8, −22.7)	−24.5 (−25.8, −21.1)	−22.8 (−25.6, −20.9)	**0.029**
3D GCS, %	−23.6 (−26.6, −19.9)	−24.9 (−26.9, −20.9)	−25.6 (−27.0, −17.1)	−26.6 (−29.1, −22.5)	−22.7 (−25.9, −19.7)	**0.031**

Data are expressed as median (Q1, Q3). 3D, three-dimensional; AEF, anteroposterior EF; AEFi, anterposterior EF index; EDV, end-diastolic volume; EF, ejection fraction; ESV, end-systolic volume; GAS, global area strain; GCS, global circumferential strain; GLS, global longitudinal strain; LEF, longitudinal EF; LEFi, longitudinal EF index; REF, radial EF; REFi, radial EF index; RV, right ventricle; RVEDVi, indexed right ventricular end-diastolic volume; RVESVi, indexed right ventricular end- systolic volume. Bolded values are statistically significant ($p < 0.05$).

4.3. The characterization of the right ventricular contraction pattern and its associations with exercise capacity in a large cohort of adolescent athletes using resting three-dimensional echocardiography

4.3.1. Basic demographic, anthropometric and hemodynamic data of the adolescent athletes and control population

Athletes had significantly higher values of height and BSA compared with the sedentary control group. Athletes also demonstrated significantly higher resting SBP and lower HR than controls, whereas DBP was similar in the two groups. Most of the athletes participated in mixed and endurance classes of sports, predominantly soccer (46.0%), water polo (33.4%), and swimming (10.2%); however, other types of sports, such as power and skill, were represented as well in our cohort of athletes (i.e., wrestling, boxing, kenpo, fencing, squash)(51). The athletes have been participating in competitive sports for 8±3 years with a training duration of 12±6 h/week at the time of the echocardiographic evaluation, and 94 out of the 215 (43.7%) participants were members of the national team in the corresponding age group (59, 64). The athlete's CPET-derived peak exercise capacity was also quantified with an average value of 54 ml/kg/min (Table 11).

Table 11. Baseline and training-specific characteristics of athlete and control groups

	Athletes (n=215)	**Controls (n=38)**	**P**
Baseline characteristics			
Age (years)	15.8±1.4	15.3±2.0	0.060
Male, n (%)	169 (78.6)	28 (73.7)	0.503
Height (cm)	175.6±10.3	169.4±11.8	0.022
Weight (kg)	67.0±12.9	61.0±10.4	0.072
BSA (m^2)	1.80±0.2	1.69±0.2	0.045
SBP (mmHg)	129.8±14.5	119.2±13.2	0.005
DBP (mmHg)	71.4±9.0	75.5±6.4	0.076
HR (bpm)	70.5±12.1	78.4±15.0	0.014
Training specific characteristics			
Type of sport			
● **Mixed, n (%)**	180 (83.7)	-	
● **Endurance, n (%)**	26 (12.1)	-	
● **Power, n (%)**	3 (1.4)	-	
● **Skill, n (%)**	6 (2.8)	-	
Since (years)	8.4±3.0	-	
Training time (h/week)	12.3±6.1	-	

VO_2 (L/min)	3.6±0.8	-
VO_2/kg (mL/kg/min)	54.4±6.9	-

Continuous variables are presented as means ± SD, categorical variables are reported as frequencies (%). BSA: body surface area, DBP: diastolic blood pressure, HR: heart rate, SBP: systolic blood pressure, VO_2: peak oxygen uptake, VO_2/kg: peak oxygen uptake indexed to body weight.

4.3.2. Conventional 2D echocardiographic parameters of athletes and controls

Left ventricular end-diastolic internal diameter, wall thicknesses, and calculated LVMi were significantly higher in athletes compared with controls. Regarding diastolic function, transmitral E-wave velocities were significantly lower in athletes. Systolic, early diastolic and atrial velocities of the mitral septal and lateral annuli were significantly lower in athletes. Concerning the right heart, RV basal diameter was larger, along with pulmonary artery systolic pressure, which also showed significantly higher values among the athlete population. In athletes, right ventricular FAC and RV FWLS showed decreased resting values (Table 12).

Table 12. Conventional 2D echocardiographic parameters of athlete and control groups

	Athletes (n=215)	**Controls (n=38)**	**P**
LVIDd (mm)	49.3±4.1	45.1±4.1	<0.001
IVSd (mm)	9.5±1.4	8.4±1.3	<0.001
PWd (mm)	8.6±1.2	7.4±1.1	<0.001
RWT (%)	0.35±0.05	0.33±0.05	0.072
LVMi (g/m^2)	86.3±15.5	66.0±12.8	<0.001
E (cm/s)	91.3±17.0	100.4±13.1	0.002
A (cm/s)	58.0±15.5	60.0±13.4	0.445
E/A	1.66±0.47	1.75±0.42	0.299
DT (ms)	168.9±33.3	161.8±34.4	0.230
Mitral lateral s′ (cm/s)	11.8±2.4	12.6±2.5	0.048
Mitral lateral e′ (cm/s)	18.2±3.0	19.5±3.4	0.017
Mitral lateral a′ (cm/s)	6.2±1.9	7.6±2.1	<0.001
Mitral medial s′ (cm/s)	9.1±1.4	9.7±1.5	0.019
Mitral medial e′ (cm/s)	13.6±2.2	15.7±2.7	<0.001
Mitral medial a′ (cm/s)	6.7±1.6	7.4±1.7	0.015
E/e′ average	5.92±1.10	5.89±0.90	0.893
LAVi (mL/m^2)	24.6±7.8	21.4±5.7	0.121
RVd (mm)	33.0±4.2	30.2±2.9	<0.001
PASP (mmHg)	23.8±4.1	19.7±4.1	<0.001

TAPSE (mm)	23.3±3.7	23.7±3.4	0.618
FAC (%)	47.7±6.1	51.9±5.9	<0.001
RVSLS (%)	-23.4±4.7	-22.4±4.1	0.229
RVFWLS (%)	-29.6±4.2	-31.4±3.7	0.017
RAVi (mL/m^2)	26.1±6.6	25.9±9.1	0.888

Continuous variables are presented as means ± SD, categorical variables are reported as frequencies (%). 2D: two-dimensional; A: mitral inflow velocity during atrial contraction, a': peak late (atrial) diastolic annular velocity, DT: deceleration time, E: early diastolic mitral inflow velocity, e': early diastolic annular velocity, FAC: fractional area change, IVSd: interventricular septal thickness at end-diastole, LAVi: left atrial volume index, LV: left ventricle, LVIDd: LV internal diameter at end-diastole, Mi: mass index, PWd: posterior wall thickness at end-diastole, RAVi: right atrial volume index, RV: right ventricle, RVd: RV basal diameter, RVFWLS: RV free wall longitudinal strain, RVSLS: RV septal longitudinal strain, PASP: pulmonary artery systolic pressure, RWT: relative wall thickness, s': systolic annular velocity, TAPSE: tricuspid annular plane systolic excursion.

4.3.3. 3D echocardiographic characteristics of athletes and controls

As expected, there were significant differences between the athlete and the control group concerning LV and RV morphological and functional parameters. Athletes demonstrated significantly higher LV and RV EDVi, ESVi and SVi values along with a significantly higher LVMi. In athletes, resting LV and RV EF values were significantly lower compared with control adolescents; however, remained within a normal range. Concerning the contraction pattern of the RV, values of REF and AEF were lower in athletes compared with controls, whereas values of LEF did not show any difference between the two groups. The relative contribution of radial (REF/RVEF, REF') and anteroposterior (AEF/RVEF, AEF') motion components to global RV function was significantly lower in athletes, whereas the relative contribution of the longitudinal (LEF/RVEF, LEF') motion component was higher compared with controls (59, 64) (Table 13).

Table 13. Three-dimensional echocardiographic data of athlete and control groups

	Athletes (n=215)	**Controls (n=38)**	**P**
LEFT VENTRICLE			

LV EDVi (mL/m^2)	80.0±13.0	64.2±9.5	<0.001
LV ESVi (mL/m^2)	34.2±7.2	25.0±5.0	<0.001
LV SVi (mL/m^2)	45.7±7.3	39.2±5.8	0.001
LV Mi (g/m^2)	83.8±13.5	67.9±13.0	<0.001
LV EF (%)	57.3±3.9	61.4±3.4	<0.001
RIGHT VENTRICLE			
RV EDVi (mL/m^2)	80.7±14.3	67.6±10.0	0.001
RV ESVi (mL/m^2)	36.3±8.5	27.6±4.2	<0.001
RV SVi (mL/m^2)	44.4±7.3	40.0±7.3	0.024
RV EF (%)	55.3±4.5	60.4±4.9	<0.001
RV LEF (%)	25.1±5.3	24.3±4.7	0.364
RV REF (%)	22.4±6.0	29.9±5.2	<0.001
RV AEF (%)	26.0±5.2	30.4±5.4	<0.001
LEF/RVEF	0.45±0.08	0.40±0.07	0.001
REF/RVEF	0.40±0.10	0.49±0.06	<0.001
AEF/RVEF	0.47±0.08	0.50±0.07	0.018
LEF' (%)	19.0±4.0	17.4±3.3	0.025
REF' (%)	16.8±4.2	21.3±3.2	<0.001
AEF' (%)	19.5±3.5	21.7±3.4	0.001

Continuous variables are presented as means ± SD, categorical variables are reported as frequencies (%). AEF: anteroposterior ejection fraction, EDVi: end-diastolic volume index, EF: ejection fraction, ESVi: end-systolic volume index, LEF: longitudinal ejection fraction, LV: left ventricle, Mi: mass index, REF: radial ejection fraction, RV: right ventricle, SVi: stroke volume index.

4.3.4. Comparison of training-specific characteristics and 3D echocardiographic data in female and male athletes

We have compared male (n = 169) and female (n = 46) athletes based on training-specific characteristics and 3D echocardiographic data. Male athletes were younger, and they have been participating in competitive sports for longer periods of time; however, females had a longer average weekly training duration. Male athletes also showed higher values of CPET-derived peak exercise capacity compared with females. Regarding the 3D echocardiographic results, specific morphological and functional differences were observed between male and female athletes. Male sex was associated with higher values of LV and RV EDVi, ESVi and SVi. Similarly, LVMi, values were higher among male athletes compared with females. In male athletes, LVEF, along with RVEF showed significantly decreased resting values compared with females. Concerning the RV mechanics, values of REF and AEF were significantly lower, whereas LEF showed higher

values in male athletes. The relative contribution of radial (REF/RVEF, REF') as well as the anteroposterior (AEF/RVEF, AEF') component was significantly lower in male athletes, while the longitudinal contribution (LEF/RVEF, LEF') was higher compared to female athletes (59, 64) (Table 14 and Figure 5).

Table 14. Comparison of training-specific characteristics and 3D echocardiographic data in female and male athletes

	Male athletes (n=169)	Female athletes (n=46)	P
Age (years)	15.6±1.4	16.4±1.2	<0.001
Since (years)	8.7±3.0	7.3±2.8	0.007
Training time (h/week)	10.7±4.7	17.9±7.1	<0.001
VO_2/kg (mL/kg/min)	56.1±6.1	48.1±5.7	<0.001
LEFT VENTRICLE			
LV EDVi (mL/m^2)	82.5±12.5	70.6±10.5	<0.001
LV ESVi (mL/m^2)	35.7±6.9	28.9±5.5	<0.001
LV SVi (mL/m^2)	46.7±7.2	41.6±6.6	<0.001
LV Mi (g/m^2)	86.2±12.8	75.1±12.4	<0.001
LV EF (%)	56.8±3.7	59.0±4.2	0.001
RIGHT VENTRICLE			
RV EDVi (mL/m^2)	83.4±13.4	70.8±13.0	<0.001
RV ESVi (mL/m^2)	37.8±8.2	30.8±7.3	<0.001
RV SVi (mL/m^2)	45.6±6.9	39.9±7.0	<0.001
RV EF (%)	55.0±4.5	56.7±4.3	0.023
RV LEF (%)	25.6±5.5	23.5±4.1	0.017
RV REF (%)	21.7±6.2	24.9±4.6	0.002
RV AEF (%)	25.5±4.9	27.9±5.9	0.005
LEF/RVEF	0.46±0.09	0.41±0.07	<0.001
REF/RVEF	0.39±0.10	0.44±0.07	0.005
AEF/RVEF	0.46±0.08	0.49±0.08	0.047
LEF' (%)	19.4±4.1	17.5±2.9	0.004
REF' (%)	16.4±4.3	18.5±3.3	0.002
AEF' (%)	19.2±3.4	20.7±3.7	0.014

Continuous variables are presented as means ± SD, categorical variables are reported as frequencies (%). 3D: three-dimensional; AEF: anteroposterior ejection fraction, EDVi: end-diastolic volume index, EF: ejection fraction, ESVi: end-systolic volume index, LEF: longitudinal ejection fraction, LV: left ventricle, Mi: mass index, REF: radial ejection fraction, RV: right ventricle, SVi: stroke volume index; VO_2/kg: peak oxygen uptake indexed to body weight.

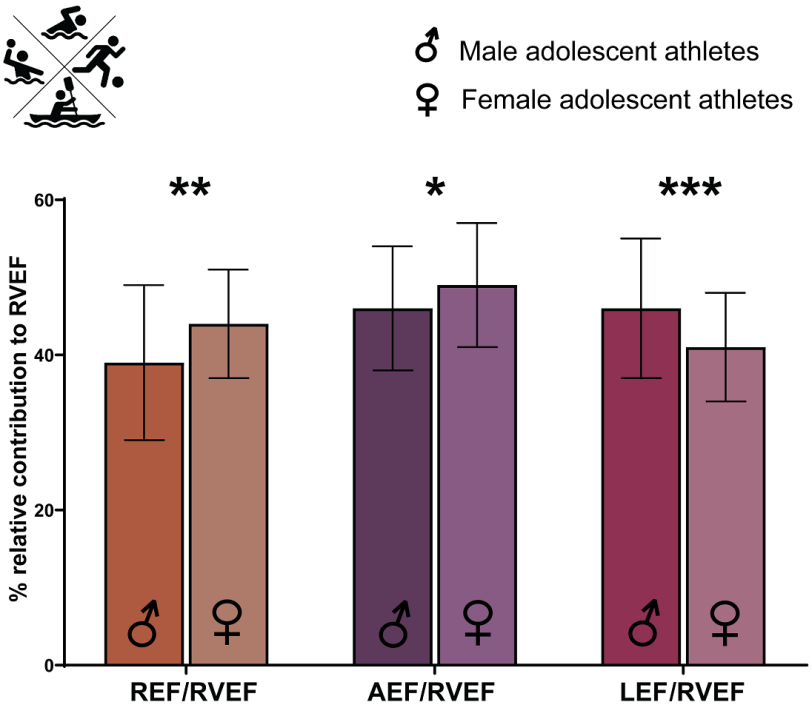

Figure 5. Sex-related differences in right ventricular (RV) contraction pattern in adolescent athletes (68). Male sex was associated with significantly lower radial contribution to RV ejection fraction (REF/RVEF) as well as anteroposterior shortening (AEF/RVEF), while the contribution of longitudinal shortening (LEF/RVEF) was higher compared to female athletes. Bars represent mean values with standard deviation.

4.3.5. Correlations between 3D echocardiography-derived parameters and VO_2/kg

Univariable correlations between 3DE-derived parameters and VO_2/kg were assessed using the athlete population. LV volumes, such as LV EDVi ($r = 0.377$, $P < 0.001$), LV ESVi ($r = 0.340$, $P < 0.001$), and LV SVi ($r = 0.344$, $P < 0.001$) as well as LV Mi ($r = 0.369$, $P < 0.001$) correlated moderately with VO_2/kg. LV EF ($r = -0.272$, $P < 0.001$) showed a weak inverse correlation with peak exercise capacity. Regarding the right heart, RV EDVi ($r = 0.377$, $P < 0.001$), RV ESVi ($r = 0.340$, $P < 0.001$), and RV SVi ($r = 0.344$, $P < 0.001$) showed moderate correlations with VO_2/kg. Right ventricular EF had no significant correlation with VO_2/kg. In terms of RV mechanics, LEF/RVEF ($r= 0.138$, $P = 0.044$) showed a weak positive correlation with VO_2/kg, while AEF/RVEF ($r= -0.155$, $P = 0.023$) showed a weak inverse correlation with it.

5. DISCUSSION

5.1. Quantifying the relative contributions of the longitudinal, radial, and anteroposterior motion components of global right ventricular function and examine their determining factors in a large cohort of healthy volunteers using 3D echocardiography

The aim of our dual-center study was to delineate the physiological contributions of RV longitudinal, radial, and anteroposterior motion to global RV function, and to explore their associations with relevant morphometric and demographic parameters. Our findings indicate that anteroposterior and longitudinal shortening are the predominant components of RV contraction. However, we observed an age-dependent shift in these dynamics: the relative contribution of radial motion increases with age, while that of longitudinal shortening decreases. Notably, after the age of 40, longitudinal and radial motion contribute equally to global RV function. Individuals over 60 years of age constitute a distinct subgroup with respect to RV contraction patterns, a difference that may be explained by the age-related elevation in PASP.

Numerous studies have demonstrated the independent prognostic value of RV morphology and function (69, 70, 71, 72, 73). Despite these robust findings, the assessment of RV geometry and function in routine clinical practice often relies on simple linear measurements, which carry inherent limitations. Conventional echocardiographic parameters such as TAPSE and FAC have shown strong correlations with RVEF and have established diagnostic and prognostic utility across various cardiovascular conditions (74, 75, 76). However, TAPSE reflects only the longitudinal motion of the RV and is subject to several sources of measurement variability. FAC, which quantifies the radial contraction of the RV free wall, similarly evaluates RV function in a single 2D imaging plane and therefore provides a limited perspective (77). In contrast, 3DE offers incremental value by allowing accurate volumetric assessment of RV morphology and function without relying on geometric assumptions, thus facilitating the definition of normative RVEF values (78). Importantly, a preserved RVEF does not necessarily exclude significant deviations from the physiological RV contraction pattern (74).

Three principal mechanisms contribute to RV ejection: (1) shortening along the longitudinal axis, characterized by apical traction of the tricuspid annulus (longitudinal

motion); (2) inward displacement of the RV free wall (radial motion); and (3) traction of the RV free wall insertion points mediated by the circumferential deformation of the LV myocardium (anteroposterior motion) (79). These distinct motion components are closely related to the underlying myocardial architecture of the RV. The RV myocardium exhibits a complex 3D arrangement of myofibers, predominantly comprising two main layers: a subendocardial layer aligned mainly in the longitudinal direction, and a subepicardial layer with a primarily circumferential orientation (13). Owing to the shared interventricular septum and the presence of myocardial fibers crossing the interventricular groove, LV contraction significantly influences RV function (22, 80).

Previous data suggested that longitudinal shortening accounts for approximately 80% of RV ejection, while the inward motion of the free wall plays only a minor role (22). However, several studies have challenged this view, emphasizing the potential significance of the "bellows" effect—radial shortening—and anteroposterior shortening in both healthy individuals and patients with cardiovascular disease (61, 74, 81, 82). While the longitudinal displacement of the tricuspid annulus is indeed prominent, it is important to note that due to the extensive surface area of the RV free wall, even minimal inward displacement can lead to substantial volume change (83). Nonetheless, current clinical practice lacks a specific RV functional parameter that exclusively quantifies the nonlongitudinal components of RV contraction. Prior studies have shown that RV circumferential deformation (the composite of radial and anteroposterior motions) exceeds longitudinal deformation, a finding that supports our results (84, 85). These observations mirror the deformation characteristics of the LV: although longitudinal shortening of the LV carries significant diagnostic and prognostic relevance, circumferential shortening contributes more substantially to LVEF (86).

We observed an age-related functional shift in RV mechanics, characterized by an increasing contribution of radial motion and a decreasing role of longitudinal shortening. Notably, this shift appears to be independent of concurrent age-related changes in RV morphology. Prior investigations utilizing Doppler tissue imaging–derived velocities and speckle-tracking echocardiography have similarly reported an age-dependent decline in RV longitudinal contraction, aligning with our findings (87, 88). Consistent with our

observations regarding LEFi, Muraru et al.(87) also identified age, LV GLS, and PASP as independent predictors of RV longitudinal performance.

Compared with longitudinal function, radial motion of the RV has been relatively underexplored in clinical research. In a pediatric study, a functional transition was documented from the neonatal period to early adulthood: the authors observed a predominance of radial systolic function in younger individuals, which progressively shifted toward dominant longitudinal shortening with increasing age. However, their analysis relied on simple linear parameters to quantify these motion components (20). Our findings indicate that, in adulthood, a less pronounced yet still notable shift occurs—characterized by a decrease in longitudinal contribution and an increase in radial motion—which may be attributed to age-related alterations in RV myofiber architecture (89).

Anteroposterior shortening of the RV is even more frequently overlooked than other motion components, and consequently, clinical data on this directional contraction are markedly limited. We hypothesize that RV anteroposterior shortening may serve as an indicator of LV contraction influence on RV function, thereby reflecting LV–RV interaction. Our research group observed comparable AEFi values between heart transplant recipients and healthy controls, as well as between elite athletes and sedentary individuals (65, 90). However, further investigations are warranted to elucidate the physiological and pathophysiological significance of RV anteroposterior shortening, particularly in patients with reduced LVEFs.

Interestingly, the oldest age category (≥60 years) exhibited a distinct RV deformation pattern. In this cohort, REFi demonstrated a negative correlation with RV afterload. Previous clinical and experimental studies have suggested that reduced RV radial shortening may serve as an early marker of elevated PASP (81, 91). Therefore, our findings may indicate early functional alterations of the RV in response to mildly increased afterload in elderly individuals (92). Clinically, this observation is particularly relevant in the context of HF with preserved EF, in which the importance of RV radial (transverse) function has been emphasized in a recent position statement by the Heart Failure Association of the European Society of Cardiology (93). In contrast to pressure

overload, a significantly increased contribution of radial motion has been observed in heart transplant recipients and patients undergoing other forms of open-heart surgery (90). These findings suggest that several additional factors may influence RV radial function, including loading conditions, pericardial constraint, and autonomic innervation (91, 94, 95).

We observed no sex-related differences in the relative contributions of the three principal components of RV contraction; however, both RV GLS and RV GCS were significantly more negative in women, which may be attributed to their lower RV volumes and higher RVEFs. In comparing the study populations from the two participating centers, we also evaluated potential racial differences. Japanese subjects exhibited significantly lower RV volume indices and RVEFs, consistent with preliminary findings from the large-scale, international World Alliance of Societies of Echocardiography study (96). Notably, the RV contraction pattern differed as well: Japanese individuals demonstrated significantly higher longitudinal and anteroposterior contributions and significantly lower radial contributions to global RV function. The final results from the World Alliance of Societies of Echocardiography study are expected to provide a more comprehensive analysis of racial differences in RV morphology and function (45, 97).

When we compared individuals in the lowest quartile of LEFi with the remainder of the study population, no significant difference in RVEF was observed; however, REFi was notably higher in this subgroup. This finding further supports the notion that reduced longitudinal function of the RV does not necessarily indicate dysfunction in all cases.

Several demographic and hemodynamic parameters showed correlations with RV morphology and deformation patterns. Similar associations of RVEDVi and RVEF with age, BSA, HR, and systemic blood pressure have been previously reported (78, 96). The inverse relationships observed between REFi and LEFi with BSA suggest that body size influences RV function, possibly due to differences in hemodynamic load (98, 99). We also identified a positive correlation between REFi and systemic blood pressure, and a negative correlation between AEFi and systemic blood pressure, underscoring the significance of ventricular interaction. Experimental data indicate that changes in LV systolic function in response to altered LV loading conditions result in reciprocal changes

in radial and anteroposterior shortening, consistent with our findings (100). Furthermore, in agreement with prior reports, RV GLS and LEFi showed no correlation with HR, whereas REFi were positively correlated, and RV GCS and AEFi was negatively correlated with HR. These results suggest that the RV longitudinal and circumferential fibers may exhibit distinct inotropic responses to HR changes, reflecting differences in the force-frequency relationship (101).

5.2. Quantifying the longitudinal, radial and anteroposterior components of global right ventricular function using 3D echocardiography in a cohort of healthy children and examine maturational changes in these parameters

The primary aim of this two-center study was to delineate the specific contributions of longitudinal, radial, and anteroposterior contraction to global RV function in a cohort of healthy children using 3D echocardiographic imaging combined with advanced analytical software. Additionally, we sought to characterize the maturational changes occurring in each RV contraction component alongside the global functional parameters. Our major finding demonstrated that while the longitudinal and radial components contributed similarly, anteroposterior contraction predominated across the overall cohort. Furthermore, age-related differences were observed in global RVEF, REF, REFi, and all measured components of RV strain.

In this study, we identified the predominance of anteroposterior shortening across nearly all age groups. Conventional 2D parameters of RV function have largely relied on simple, linear measurements that incompletely capture the complex mechanics of RV contraction. For instance, TAPSE, which quantifies longitudinal motion of the RV, has been shown to correlate with global RVEF and has been utilized in children with pulmonary hypertension both with and without congenital heart disease (102). FAC reflects both radial contraction of the free wall and longitudinal traction of the tricuspid annulus and has been linked to RV functional changes in patients with Ebstein anomaly undergoing the cone procedure (103). While these methods provide some quantitative insight into RV function, they remain limited as they do not comprehensively assess all axes of RV motion, notably failing to evaluate the anteroposterior contraction—which, in our study, was found to be predominant.

As previously discussed, earlier studies using 2D echocardiography have demonstrated that the RV contraction pattern in children undergoes significant changes during the first year of life, corresponding to the transition from fetal circulation—where the RV is subjected to high afterload—to postnatal circulation, characterized by a gradual decline in pulmonary vascular resistance over the initial months. One study employing TAPSE and a surrogate marker of radial contraction identified a clear shift from predominantly radial to more longitudinal contraction around 4 months of age (104). Although likely underpowered to detect significant differences in radial contraction between neonates (under 1 month) and older children, our findings indicate age-related changes in the contribution of radial shortening. Other researchers using 2D speckle-tracking strain analysis reported an increase in longitudinal contraction during the first year of life in premature infants (104). In contrast, our data suggest a more complex pattern, with an early increase in longitudinal shortening magnitude followed by a subsequent return to baseline values. Importantly, we are the first to characterize anteroposterior contraction patterns in children. This anteroposterior shortening is largely driven by circumferential shortening of the LV mid-layer myofibers, which draw the RV free-wall insertion points closer together. Previous studies have demonstrated a strong association between AEFi and LVEF in both healthy individuals and patients with congenital heart disease resulting in a systemic RV (105, 106).

The maturational differences in directional RV contraction identified in this study underscore the importance of utilizing advanced echocardiographic techniques to evaluate RV contraction patterns in children with both simple and complex congenital heart disease. Previous studies have demonstrated the prognostic significance of global RV function in this population (107, 108). However, even when global RV function is preserved, notable variations in the relative contributions of the three principal contraction components have been observed, as reported in adults undergoing mitral valve surgery and in patients with volume- or pressure-loading lesions affecting the right heart (61, 105, 109). Quantifying and understanding the relative contributions of each RV contraction component may have important clinical applications across various subsets of RV pathology by providing insight into the long-term effects of: (1) pressure overload in children with chronic RV outflow tract obstruction (e.g., tetralogy of Fallot, congenital pulmonic stenosis, idiopathic pulmonary arterial hypertension); (2) volume overload in

children with longstanding left-to-right shunts (e.g., partial anomalous pulmonary venous connections, atrial septal defects); (3) primary RV myopathies such as arrhythmogenic cardiomyopathy; and (4) complex anatomies requiring the RV to function as the systemic ventricle, whether in single-ventricle circulations (e.g., hypoplastic left heart syndrome) or biventricular circulations (e.g., "congenitally corrected" transposition of the great arteries). A more nuanced understanding of the evolution and progression of RV contraction changes could aid clinicians in assessing the impact of medical therapies and refining the timing of procedural interventions.

5.3. The characterization of the right ventricular contraction pattern and its associations with exercise capacity in a large cohort of adolescent athletes using resting three-dimensional echocardiography

To the best of our knowledge, this is the first study specifically designed to investigate the adolescent athlete's heart using advanced 3DE and to examine its relationship with exercise capacity, as assessed by same-day CPET. Our principal findings are as follows: (i) adolescent athletes already exhibit echocardiographic characteristics typically observed in adult athletic hearts; (ii) the right ventricular contraction pattern shifts toward a predominantly longitudinal motion (representative cases are shown in Figure 6); and (iii) biventricular morphological and functional remodeling—including the altered RV contraction pattern—demonstrates weak to moderate correlations with peak exercise capacity as measured by CPET.

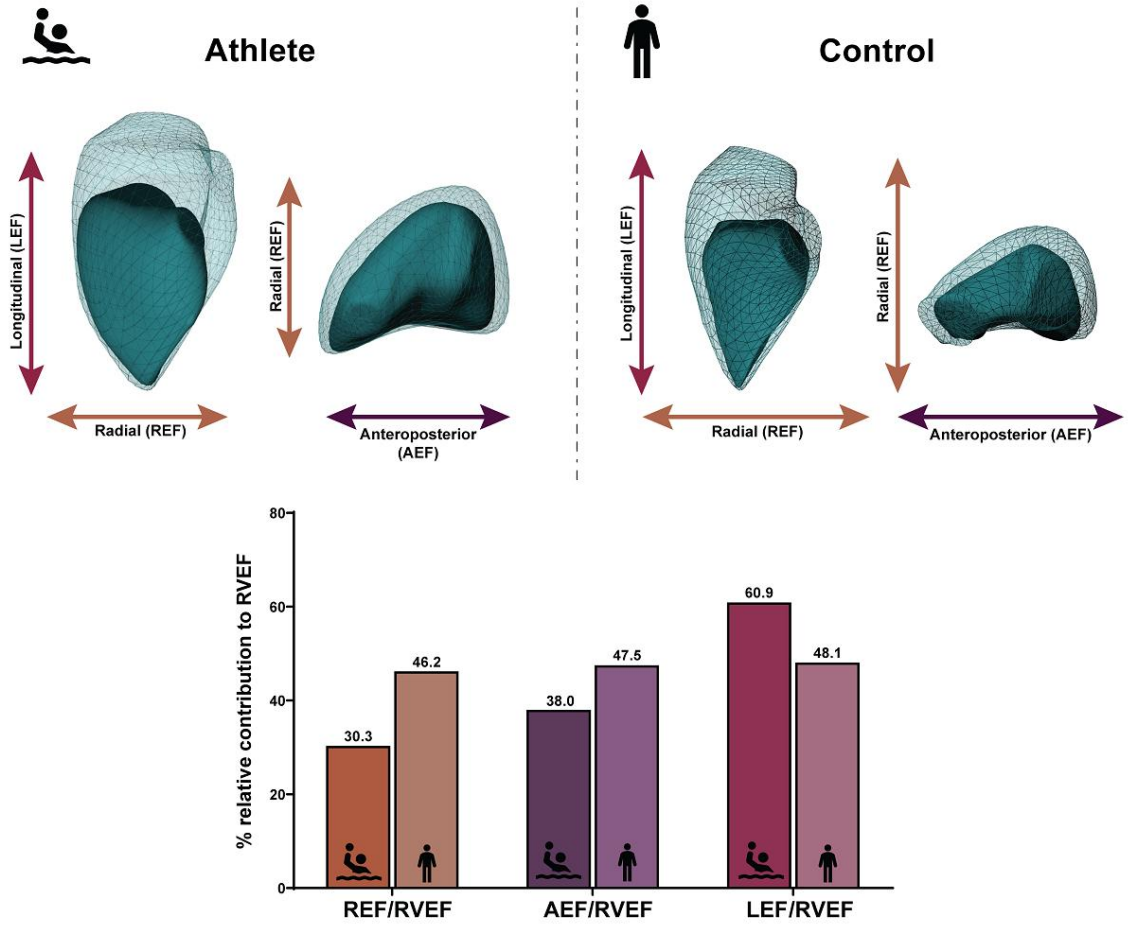

Figure 6. Graphical representation of an elite adolescent water polo athlete versus a healthy, sedentary volunteer, in terms of 3D right ventricular (RV) contraction patterns (68). The relative contributions of radial (REF') and anteroposterior (AEF') motion components to overall RV function were significantly lower in the athlete, whereas the relative contribution of the longitudinal (LEF') motion component was higher compared with the control child.

Historically, there has been debate regarding whether classical features of the athlete's heart can manifest during childhood. However, recent evidence clearly demonstrates that pediatric individuals also lie on the phenotypic spectrum. A recent systematic review and meta-analysis confirmed an approximate 27% increase in LV M, accompanied by less pronounced but statistically significant increases in LV and left atrial dimensions (110). Our findings align with these observations, regardless of the imaging modality employed—be it conventional or 3DE. Moreover, morphological changes in the LV induced by exercise can develop rapidly during adolescence; one study demonstrated LV

remodeling after just 10 weeks of supervised endurance training (8–10 hours per week) (111). Another investigation revealed that, similar to other exercise-naïve age groups, pre-adolescent athletes initially exhibit concentric hypertrophy, which subsequently transitions to an excentric pattern with continued training (112). Adolescence represents a physiologically dynamic and anabolic period, exerting substantial influence on cardiovascular development, which may act synergistically with physical training stimuli (113, 114). Understanding the development and regression dynamics of exercise-induced cardiac remodeling remains a central issue in sports cardiology, with important implications for both differential diagnosis and long-term prognosis (115). These challenges become even more complex in pediatric populations, underscoring the need for large-scale, longitudinal studies in this age group. Nonetheless, a growing body of evidence supports that significant structural and functional cardiac adaptations occur in both male and female adolescent athletes (57, 110, 111, 116, 117).

Owing largely to the challenges of accurate assessment using conventional imaging methods, our understanding of the RV remains more limited compared to the LV. Nevertheless, prior studies have shown that as little as five months of training can lead to a more pronounced RV dilation than what is typically observed in non-athletic children through natural growth alone (116). Additionally, RV size has been associated with the number of weekly training hours (112). Endurance-trained adolescents have been found to exhibit increased RV longitudinal function, as assessed by TAPSE and tissue Doppler imagine (TDI) derived s′ velocity (117). Our findings corroborate and extend these results through the use of advanced imaging modalities, particularly 3DE-based volumetric models. Importantly, this relative enhancement in longitudinal shortening is accompanied by reductions in both radial and anteroposterior shortening. This mechanical shift in RV contraction has previously been observed in adult water polo athletes, where it was also associated with superior exercise capacity (65). We hypothesize that these adaptations are the result of exercise-induced changes in myofiber orientation, favoring a more oblique and longitudinal alignment (118). Consequently, longitudinal shortening becomes the predominant component of RV function, while radial shortening (reflecting inward motion of the RV free wall) and anteroposterior shortening (mediated by LV-induced traction of the RV free wall) are relatively diminished. Our study is the first to demonstrate that this specific RV mechanical adaptation is already present in adolescent

athletes, and that it remains linked to improved exercise performance. Notably, we employed 3DE to quantify both LV and RV volumes and mechanics—an approach that adds significant value over traditional methods. Most recently, Jones et al. provided sex-specific pediatric reference values for RV volumes, EF, and z-score equations using 3DE across five North American centers (119). The RV volumes observed in our athletic cohort were markedly higher, indicating substantial remodeling not only of the left heart but also of the right heart (120). Importantly, these features were also evident in female adolescent athletes, albeit to a lesser degree. Therefore, female athletes should be equally considered within the spectrum of exercise-induced cardiac adaptation. Moreover, emerging data suggest that the classical Morganroth hypothesis—which posits concentric hypertrophy in strength-trained athletes and eccentric hypertrophy in endurance-trained athletes—also applies to the female athlete's heart (121). Taken together, these findings highlight the importance of contextualizing athletic cardiac remodeling across sex and age groups. During clinical evaluation, any apparent "outlier" findings—such as disproportionately elevated ventricular volumes or LV M in a moderately trained or amateur athlete—should prompt further investigation with advanced diagnostic modalities, including stress testing, cardiac MRI, and genetic testing, to rule out underlying cardiomyopathies or other pathologies.

Importantly, the phenotypic features of various cardiac pathologies often overlap with those observed in the normal athletic heart, making differentiation particularly challenging (122). This challenge is amplified in pediatric populations, where additional confounding variables—such as sex differences, biological maturation, and somatic growth—complicate the interpretation of cardiac findings (57). As such, a comprehensive understanding of the physiological characteristics of the healthy pediatric athlete's heart is a critical prerequisite for both future research and accurate clinical evaluation. Traditional tools such as physical examination, family history, and ECG, while valuable, often lack the resolution necessary to discern subtle structural or functional abnormalities. In this context, echocardiography is gaining increasing prominence as an essential screening modality within clinical protocols. Nevertheless, advanced echocardiographic techniques—such as speckle-tracking and 3DE—remain underutilized in sports medicine, despite their growing adoption in cardiology and their superior ability to characterize both geometry and mechanics of the heart (46). 3DE, in particular, enables

detailed assessment of the morphological and functional features of the athlete's heart, even under resting conditions, and has shown meaningful correlations with exercise capacity. These capabilities highlight its potential as a powerful diagnostic tool. Our current findings support the continued integration of advanced echocardiographic modalities into the evaluation of adolescent athletes. Future research should aim to validate their utility in distinguishing physiological remodeling from early or subclinical manifestations of cardiac disease, thereby improving diagnostic accuracy and guiding clinical decision-making in this unique population.

5.4. Limitations

In our first study, we included a relatively large cohort of healthy subjects with balanced sex and age distribution, allowing comparison between European and Japanese individuals. However, other racial differences could not be assessed, and further multiethnic expansion may strengthen our findings. Subjects >60 years were grouped together despite a broader age range. As no reference standard exists for assessing RV longitudinal, radial, and anteroposterior motions, our results could not be validated against a gold standard. REFi showed greater variability, likely reflecting higher heterogeneity in RV free wall inward motion. The clinical value of RV motion decomposition remains to be determined, as data on its diagnostic and prognostic relevance are limited. Our method yields multiplicative, not additive, contributions; thus, the sum of directional components exceeds 100%.

In our second study, the study cohort was limited by a smaller number of subjects in the younger age groups—an important consideration given the substantial hemodynamic changes the RV undergoes in the early postnatal period. Additionally, recruitment strategies resulted in a male predominance in the oldest age group, with all but 9 subjects at the Semmelweis site being male. Consequently, our exploratory analysis aimed at detecting sex-specific differences in EF parameters across age groups was likely underpowered.

Our third study was a single-center, retrospective, cross-sectional investigation involving a limited number of adolescent athletes. Nonetheless, the application of advanced echocardiographic techniques combined with same-day CPET enhances its value. Due to

the relatively small cohort, we were unable to assess differences across sport types or ethnic groups. Female athletes were underrepresented, and their somewhat different characteristics (e.g., older age, higher weekly training volume) further limited sex-based comparisons. Additionally, some of the youngest male athletes may not have yet begun their adolescent growth spurt. Finally, although we lacked a gold standard comparison, all post-processing software used has been extensively validated against CMR (39, 41).

6. CONCLUSIONS

In our first study, we demonstrated that the often-overlooked radial and anteroposterior motion components of the RV are as important as longitudinal shortening in determining global RV function in healthy individuals. These findings highlight the value of 3DE in evaluating RV performance. Clinical data indicate that normal values of parameters reflecting only longitudinal motion do not rule out RV dysfunction, just as preserved global RV function can coexist with abnormal longitudinal indices. 3D RVEF captures the integrated contribution of all motion directions, potentially offering superior diagnostic and prognostic utility compared to conventional M-mode or 2D techniques. Even with preserved global function, the proportional contributions of the three components may vary in specific clinical settings (e.g., RV volume or pressure overload, cardiomyopathies, left-sided HF). Thus, further research is needed to determine whether quantifying RV deformation patterns by separating longitudinal, radial, and anteroposterior components enhances the established value of RVEF.

In our second study, we found that analyzing the components of RV contraction in healthy children using 3DE is both feasible and reliable. Within this pediatric cohort, the anteroposterior component consistently exceeded both radial and longitudinal contributions. We also observed age-related changes in global RVEF and in the radial component of RV contraction. These findings support the potential of future 3DE-based investigations in pediatric populations—particularly those with congenital heart disease—to improve the detection of RV dysfunction and aid in evaluating treatment outcomes.

In our third study, we investigated a large cohort of adolescent athletes using advanced echocardiographic techniques alongside CPET. We found that both conventional and emerging features of the athlete's heart—including specific alterations in RV contraction patterns—are already present in pediatric athletes and correlate with peak exercise capacity. Further research using advanced imaging modalities in pediatric populations is warranted to help differentiate the healthy adolescent athlete's heart from rare pathological conditions with overlapping phenotypes.

7. SUMMARY

Due to the complex anatomy of the RV, 2D echocardiography has limited utility in its assessment, whereas 3DE offers more accurate and reproducible quantification of RV volumes and EF. In our first study on healthy volunteers using 3DE, we demonstrated that, in addition to longitudinal motion, radial and anteroposterior components significantly contribute to global RV function, indicating that reliance solely on longitudinal parameters may be inadequate.

Accurate assessment of RV morphology and function is crucial in cardiovascular disease among children and adolescents, especially in complex congenital heart conditions. In our second study, we quantified the longitudinal, radial, and anteroposterior components of global RV function using 3DE in healthy children and evaluated maturational changes. We found age-related differences in RV contraction patterns, with anteroposterior shortening being the dominant component. Assessing 3D RV parameters in children is feasible and improves understanding of RV function, potentially enhancing detection of dysfunction and treatment evaluation in the future.

Regular intense exercise imposes significant hemodynamic demands that drive structural and functional cardiac adaptations. Pediatric athletes form a unique group where clinical interpretation is challenging due to limited data. Our third study aimed to characterize RV contraction patterns in a large cohort of adolescent athletes using resting 3DE. Similar to adults, adolescent athletes show higher biventricular volumes, reduced resting functional measures, and enhanced RV longitudinal shortening. These exercise-induced cardiac changes are already evident during adolescence.

8. REFERENCES

1. Ansari Ramandi MM, van Melle JP, Gorter TM, Hoendermis ES, van Veldhuisen DJ, Nauta JF, van der Wal MHL, Warink-Riemersma J, Voors AA, Dickinson MG. Right ventricular dysfunction in patients with new-onset heart failure: longitudinal follow-up during guideline-directed medical therapy. Eur J Heart Fail. 2022;24(12):2226-34.
2. Konstam MA, Kiernan MS, Bernstein D, Bozkurt B, Jacob M, Kapur NK, Kociol RD, Lewis EF, Mehra MR, Pagani FD, Raval AN, Ward C, American Heart Association Council on Clinical C, Council on Cardiovascular Disease in the Y, Council on Cardiovascular S, Anesthesia. Evaluation and Management of Right-Sided Heart Failure: A Scientific Statement From the American Heart Association. Circulation. 2018;137(20):e578-e622.
3. Diller GP, Radojevic J, Kempny A, Alonso-Gonzalez R, Emmanouil L, Orwat S, Swan L, Uebing A, Li W, Dimopoulos K, Gatzoulis MA, Baumgartner H. Systemic right ventricular longitudinal strain is reduced in adults with transposition of the great arteries, relates to subpulmonary ventricular function, and predicts adverse clinical outcome. Am Heart J. 2012;163(5):859-66.
4. Shafer KM, Mann N, Hehn R, Ubeda Tikkanen A, Valente AM, Geva T, Gauthier N, Rhodes J. Relationship between Exercise Parameters and Noninvasive Indices of Right Ventricular Function in Patients with Biventricular Circulation and Systemic Right Ventricle. Congenit Heart Dis. 2015;10(5):457-65.
5. Filippov AA, Del Nido PJ, Vasilyev NV. Management of Systemic Right Ventricular Failure in Patients With Congenitally Corrected Transposition of the Great Arteries. Circulation. 2016;134(17):1293-302.
6. Valente AM, Gauvreau K, Assenza GE, Babu-Narayan SV, Schreier J, Gatzoulis MA, Groenink M, Inuzuka R, Kilner PJ, Koyak Z, Landzberg MJ, Mulder B, Powell AJ, Wald R, Geva T. Contemporary predictors of death and sustained ventricular tachycardia in patients with repaired tetralogy of Fallot enrolled in the INDICATOR cohort. Heart. 2014;100(3):247-53.
7. Geva T, Mulder B, Gauvreau K, Babu-Narayan SV, Wald RM, Hickey K, Powell AJ, Gatzoulis MA, Valente AM. Preoperative Predictors of Death and Sustained Ventricular Tachycardia After Pulmonary Valve Replacement in Patients With Repaired

Tetralogy of Fallot Enrolled in the INDICATOR Cohort. Circulation. 2018;138(19):2106-15.

8. Driessen MMP, Meijboom FJ, Hui W, Dragulescu A, Mertens L, Friedberg MK. Regional right ventricular remodeling and function in children with idiopathic pulmonary arterial hypertension vs those with pulmonary valve stenosis: Insights into mechanics of right ventricular dysfunction. Echocardiography. 2017;34(6):888-97.

9. Jone PN, Duchateau N, Pan Z, Ivy DD, Moceri P. Right ventricular area strain from 3-dimensional echocardiography: Mechanistic insight of right ventricular dysfunction in pediatric pulmonary hypertension. J Heart Lung Transplant. 2021;40(2):138-48.

10. Haddad F, Hunt SA, Rosenthal DN, Murphy DJ. Right ventricular function in cardiovascular disease, part I: Anatomy, physiology, aging, and functional assessment of the right ventricle. Circulation. 2008;117(11):1436-48.

11. Sanz J, Sanchez-Quintana D, Bossone E, Bogaard HJ, Naeije R. Anatomy, Function, and Dysfunction of the Right Ventricle: JACC State-of-the-Art Review. J Am Coll Cardiol. 2019;73(12):1463-82.

12. Ho SY, Nihoyannopoulos P. Anatomy, echocardiography, and normal right ventricular dimensions. Heart. 2006;92 Suppl 1(Suppl 1):i2-13.

13. Dell'Italia LJ. The right ventricle: anatomy, physiology, and clinical importance. Curr Probl Cardiol. 1991;16(10):653-720.

14. Hopkins WE, Waggoner AD. Severe pulmonary hypertension without right ventricular failure: the unique hearts of patients with Eisenmenger syndrome. Am J Cardiol. 2002;89(1):34-8.

15. Rudolph AM. The changes in the circulation after birth. Their importance in congenital heart disease. Circulation. 1970;41(2):343-59.

16. Rudolph AM. The fetal circulation and its adjustments after birth in congenital heart disease. UCLA Forum Med Sci. 1970;10:105-18.

17. Davidson WR, Jr., Fee EC. Influence of aging on pulmonary hemodynamics in a population free of coronary artery disease. Am J Cardiol. 1990;65(22):1454-8.

18. Dib JC, Abergel E, Rovani C, Raffoul H, Diebold B. The age of the patient should be taken into account when interpreting Doppler assessed pulmonary artery pressures. J Am Soc Echocardiogr. 1997;10(1):72-3.

19. Klein AL, Burstow DJ, Tajik AJ, Zachariah PK, Taliercio CP, Taylor CL, Bailey KR, Seward JB. Age-related prevalence of valvular regurgitation in normal subjects: a comprehensive color flow examination of 118 volunteers. J Am Soc Echocardiogr. 1990;3(1):54-63.

20. Hashimoto I, Watanabe K. Alternation of right ventricular contraction pattern in healthy children-shift from radial to longitudinal direction at approximately 15 mm of tricuspid annular plane systolic excursion. Circ J. 2014;78(8):1967-73.

21. Cotella JI, Kovacs A, Addetia K, Fabian A, Asch FM, Lang RM, Investigators W. Three-dimensional echocardiographic evaluation of longitudinal and non-longitudinal components of right ventricular contraction: results from the World Alliance of Societies of Echocardiography study. Eur Heart J Cardiovasc Imaging. 2024;25(2):152-60.

22. Buckberg G, Hoffman JI. Right ventricular architecture responsible for mechanical performance: unifying role of ventricular septum. J Thorac Cardiovasc Surg. 2014;148(6):3166-71 e1-4.

23. Geva T, Powell AJ, Crawford EC, Chung T, Colan SD. Evaluation of regional differences in right ventricular systolic function by acoustic quantification echocardiography and cine magnetic resonance imaging. Circulation. 1998;98(4):339-45.

24. Kukulski T, Hubbert L, Arnold M, Wranne B, Hatle L, Sutherland GR. Normal regional right ventricular function and its change with age: a Doppler myocardial imaging study. J Am Soc Echocardiogr. 2000;13(3):194-204.

25. Rudski LG, Lai WW, Afilalo J, Hua L, Handschumacher MD, Chandrasekaran K, Solomon SD, Louie EK, Schiller NB. Guidelines for the echocardiographic assessment of the right heart in adults: a report from the American Society of Echocardiography endorsed by the European Association of Echocardiography, a registered branch of the European Society of Cardiology, and the Canadian Society of Echocardiography. J Am Soc Echocardiogr. 2010;23(7):685-713; quiz 86-8.

26. Forfia PR, Fisher MR, Mathai SC, Housten-Harris T, Hemnes AR, Borlaug BA, Chamera E, Corretti MC, Champion HC, Abraham TP, Girgis RE, Hassoun PM. Tricuspid annular displacement predicts survival in pulmonary hypertension. Am J Respir Crit Care Med. 2006;174(9):1034-41.

27. Ghio S, Klersy C, Magrini G, D'Armini AM, Scelsi L, Raineri C, Pasotti M, Serio A, Campana C, Vigano M. Prognostic relevance of the echocardiographic assessment of

right ventricular function in patients with idiopathic pulmonary arterial hypertension. Int J Cardiol. 2010;140(3):272-8.

28. Sato T, Tsujino I, Ohira H, Oyama-Manabe N, Yamada A, Ito YM, Goto C, Watanabe T, Sakaue S, Nishimura M. Validation study on the accuracy of echocardiographic measurements of right ventricular systolic function in pulmonary hypertension. J Am Soc Echocardiogr. 2012;25(3):280-6.

29. Pavlicek M, Wahl A, Rutz T, de Marchi SF, Hille R, Wustmann K, Steck H, Eigenmann C, Schwerzmann M, Seiler C. Right ventricular systolic function assessment: rank of echocardiographic methods vs. cardiac magnetic resonance imaging. Eur J Echocardiogr. 2011;12(11):871-80.

30. Sachdev A, Villarraga HR, Frantz RP, McGoon MD, Hsiao JF, Maalouf JF, Ammash NM, McCully RB, Miller FA, Pellikka PA, Oh JK, Kane GC. Right ventricular strain for prediction of survival in patients with pulmonary arterial hypertension. Chest. 2011;139(6):1299-309.

31. Haeck ML, Scherptong RW, Marsan NA, Holman ER, Schalij MJ, Bax JJ, Vliegen HW, Delgado V. Prognostic value of right ventricular longitudinal peak systolic strain in patients with pulmonary hypertension. Circ Cardiovasc Imaging. 2012;5(5):628-36.

32. Focardi M, Cameli M, Carbone SF, Massoni A, De Vito R, Lisi M, Mondillo S. Traditional and innovative echocardiographic parameters for the analysis of right ventricular performance in comparison with cardiac magnetic resonance. Eur Heart J Cardiovasc Imaging. 2015;16(1):47-52.

33. Anavekar NS, Gerson D, Skali H, Kwong RY, Yucel EK, Solomon SD. Two-dimensional assessment of right ventricular function: an echocardiographic-MRI correlative study. Echocardiography. 2007;24(5):452-6.

34. Anavekar NS, Skali H, Bourgoun M, Ghali JK, Kober L, Maggioni AP, McMurray JJ, Velazquez E, Califf R, Pfeffer MA, Solomon SD. Usefulness of right ventricular fractional area change to predict death, heart failure, and stroke following myocardial infarction (from the VALIANT ECHO Study). Am J Cardiol. 2008;101(5):607-12.

35. Austin C, Alassas K, Burger C, Safford R, Pagan R, Duello K, Kumar P, Zeiger T, Shapiro B. Echocardiographic assessment of estimated right atrial pressure and size predicts mortality in pulmonary arterial hypertension. Chest. 2015;147(1):198-208.

36. Peyrou J, Chauvel C, Pathak A, Simon M, Dehant P, Abergel E. Preoperative right ventricular dysfunction is a strong predictor of 3 years survival after cardiac surgery. Clin Res Cardiol. 2017;106(9):734-42.
37. Mertens LL, Friedberg MK. Imaging the right ventricle--current state of the art. Nat Rev Cardiol. 2010;7(10):551-63.
38. Surkova E, Muraru D, Iliceto S, Badano LP. The use of multimodality cardiovascular imaging to assess right ventricular size and function. Int J Cardiol. 2016;214:54-69.
39. Muraru D, Spadotto V, Cecchetto A, Romeo G, Aruta P, Ermacora D, Jenei C, Cucchini U, Iliceto S, Badano LP. New speckle-tracking algorithm for right ventricular volume analysis from three-dimensional echocardiographic data sets: validation with cardiac magnetic resonance and comparison with the previous analysis tool. Eur Heart J Cardiovasc Imaging. 2016;17(11):1279-89.
40. Lang RM, Badano LP, Mor-Avi V, Afilalo J, Armstrong A, Ernande L, Flachskampf FA, Foster E, Goldstein SA, Kuznetsova T, Lancellotti P, Muraru D, Picard MH, Rietzschel ER, Rudski L, Spencer KT, Tsang W, Voigt JU. Recommendations for cardiac chamber quantification by echocardiography in adults: an update from the American Society of Echocardiography and the European Association of Cardiovascular Imaging. J Am Soc Echocardiogr. 2015;28(1):1-39 e14.
41. Tokodi M, Staub L, Budai A, Lakatos BK, Csakvari M, Suhai FI, Szabo L, Fabian A, Vago H, Toser Z, Merkely B, Kovacs A. Partitioning the Right Ventricle Into 15 Segments and Decomposing Its Motion Using 3D Echocardiography-Based Models: The Updated ReVISION Method. Front Cardiovasc Med. 2021;8:622118.
42. Mitchell C, Rahko PS, Blauwet LA, Canaday B, Finstuen JA, Foster MC, Horton K, Ogunyankin KO, Palma RA, Velazquez EJ. Guidelines for Performing a Comprehensive Transthoracic Echocardiographic Examination in Adults: Recommendations from the American Society of Echocardiography. J Am Soc Echocardiogr. 2019;32(1):1-64.
43. Lang RM, Badano LP, Mor-Avi V, Afilalo J, Armstrong A, Ernande L, Flachskampf FA, Foster E, Goldstein SA, Kuznetsova T, Lancellotti P, Muraru D, Picard MH, Rietzschel ER, Rudski L, Spencer KT, Tsang W, Voigt JU. Recommendations for cardiac chamber quantification by echocardiography in adults: an update from the

American Society of Echocardiography and the European Association of Cardiovascular Imaging. Eur Heart J Cardiovasc Imaging. 2015;16(3):233-70.

44. Lopez L, Saurers DL, Barker PCA, Cohen MS, Colan SD, Dwyer J, Forsha D, Friedberg MK, Lai WW, Printz BF, Sachdeva R, Soni-Patel NR, Truong DT, Young LT, Altman CA. Guidelines for Performing a Comprehensive Pediatric Transthoracic Echocardiogram: Recommendations From the American Society of Echocardiography. J Am Soc Echocardiogr. 2024;37(2):119-70.

45. Asch FM, Miyoshi T, Addetia K, Citro R, Daimon M, Desale S, Fajardo PG, Kasliwal RR, Kirkpatrick JN, Monaghan MJ, Muraru D, Ogunyankin KO, Park SW, Ronderos RE, Sadeghpour A, Scalia GM, Takeuchi M, Tsang W, Tucay ES, Tude Rodrigues AC, Vivekanandan A, Zhang Y, Blitz A, Lang RM, Investigators W. Similarities and Differences in Left Ventricular Size and Function among Races and Nationalities: Results of the World Alliance Societies of Echocardiography Normal Values Study. J Am Soc Echocardiogr. 2019;32(11):1396-406 e2.

46. Fabian A, Ujvari A, Tokodi M, Lakatos BK, Kiss O, Babity M, Zamodics M, Sydo N, Csulak E, Vago H, Szabo L, Kiss AR, Szucs A, Hizoh I, Merkely B, Kovacs A. Biventricular mechanical pattern of the athlete's heart: comprehensive characterization using three-dimensional echocardiography. Eur J Prev Cardiol. 2022;29(12):1594-604.

47. Morganroth J, Maron BJ, Henry WL, Epstein SE. Comparative left ventricular dimensions in trained athletes. Ann Intern Med. 1975;82(4):521-4.

48. Prior DL, La Gerche A. The athlete's heart. Heart. 2012;98(12):947-55.

49. Baggish AL, Wood MJ. Athlete's heart and cardiovascular care of the athlete: scientific and clinical update. Circulation. 2011;123(23):2723-35.

50. Haskell WL, Lee IM, Pate RR, Powell KE, Blair SN, Franklin BA, Macera CA, Heath GW, Thompson PD, Bauman A. Physical activity and public health: updated recommendation for adults from the American College of Sports Medicine and the American Heart Association. Med Sci Sports Exerc. 2007;39(8):1423-34.

51. Pelliccia A, Caselli S, Sharma S, Basso C, Bax JJ, Corrado D, D'Andrea A, D'Ascenzi F, Di Paolo FM, Edvardsen T, Gati S, Galderisi M, Heidbuchel H, Nchimi A, Nieman K, Papadakis M, Pisicchio C, Schmied C, Popescu BA, Habib G, Grobbee D, Lancellotti P, Internal reviewers for E, Eacvi. European Association of Preventive Cardiology (EAPC) and European Association of Cardiovascular Imaging (EACVI) joint

position statement: recommendations for the indication and interpretation of cardiovascular imaging in the evaluation of the athlete's heart. Eur Heart J. 2018;39(21):1949-69.

52. La Gerche A, Burns AT, Mooney DJ, Inder WJ, Taylor AJ, Bogaert J, Macisaac AI, Heidbuchel H, Prior DL. Exercise-induced right ventricular dysfunction and structural remodelling in endurance athletes. Eur Heart J. 2012;33(8):998-1006.

53. D'Andrea A, Riegler L, Golia E, Cocchia R, Scarafile R, Salerno G, Pezzullo E, Nunziata L, Citro R, Cuomo S, Caso P, Di Salvo G, Cittadini A, Russo MG, Calabro R, Bossone E. Range of right heart measurements in top-level athletes: the training impact. Int J Cardiol. 2013;164(1):48-57.

54. La Gerche A, Heidbuchel H, Burns AT, Mooney DJ, Taylor AJ, Pfluger HB, Inder WJ, Macisaac AI, Prior DL. Disproportionate exercise load and remodeling of the athlete's right ventricle. Med Sci Sports Exerc. 2011;43(6):974-81.

55. Oxborough D, Birch K, Shave R, George K. "Exercise-induced cardiac fatigue"--a review of the echocardiographic literature. Echocardiography. 2010;27(9):1130-40.

56. Forsa MI, Bjerring AW, Haugaa KH, Smedsrud MK, Sarvari SI, Landgraff HW, Hallen J, Edvardsen T. Young athlete's growing heart: sex differences in cardiac adaptation to exercise training during adolescence. Open Heart. 2023;10(1).

57. Ragazzoni GL, Cavigli L, Cavarretta E, Maffei S, Mandoli GE, Pastore MC, Valente S, Focardi M, Cameli M, Di Salvo G, Pieles G, D'Ascenzi F. How to evaluate resting ECG and imaging in children practising sport: a critical review and proposal of an algorithm for ECG interpretation. Eur J Prev Cardiol. 2023;30(5):375-83.

58. Mosteller RD. Simplified calculation of body-surface area. N Engl J Med. 1987;317(17):1098.

59. Kovács A. Clinical perspectives of right ventricular function as assessed by three-dimensional echocardiography 2025 [Available from: https://real-d.mtak.hu/1692/13/kovatti87_134_23_doktori_mu.pdf.

60. Lai WW, Geva T, Shirali GS, Frommelt PC, Humes RA, Brook MM, Pignatelli RH, Rychik J, Task Force of the Pediatric Council of the American Society of E, Pediatric Council of the American Society of E. Guidelines and standards for performance of a pediatric echocardiogram: a report from the Task Force of the Pediatric Council of the American Society of Echocardiography. J Am Soc Echocardiogr. 2006;19(12):1413-30.

61. Tokodi M, Nemeth E, Lakatos BK, Kispal E, Toser Z, Staub L, Racz K, Soltesz A, Szigeti S, Varga T, Gal J, Merkely B, Kovacs A. Right ventricular mechanical pattern in patients undergoing mitral valve surgery: a predictor of post-operative dysfunction? ESC Heart Fail. 2020;7(3):1246-56.

62. Lakatos BK, Nabeshima Y, Tokodi M, Nagata Y, Tősér Z, Otani K, Kitano T, Fábián A, Ujvári A, Boros AM, Merkely B, Kovács A, Takeuchi M. Importance of Nonlongitudinal Motion Components in Right Ventricular Function: Three-Dimensional Echocardiographic Study in Healthy Volunteers. J Am Soc Echocardiogr. 2020;33(8):995-1005.e1.

63. Bunting KV, Steeds RP, Slater K, Rogers JK, Gkoutos GV, Kotecha D. A Practical Guide to Assess the Reproducibility of Echocardiographic Measurements. J Am Soc Echocardiogr. 2019;32(12):1505-15.

64. Kovács A. Clinical perspectives of right ventricular function as assessed by three-dimensional echocardiography 2025.

65. Lakatos BK, Kiss O, Tokodi M, Toser Z, Sydo N, Merkely G, Babity M, Szilagyi M, Komocsin Z, Bognar C, Kovacs A, Merkely B. Exercise-induced shift in right ventricular contraction pattern: novel marker of athlete's heart? Am J Physiol Heart Circ Physiol. 2018;315(6):H1640-H8.

66. Babity M, Zamodics M, Konig A, Kiss AR, Horvath M, Gregor Z, Rakoczi R, Kovacs E, Fabian A, Tokodi M, Sydo N, Csulak E, Juhasz V, Lakatos BK, Vago H, Kovacs A, Merkely B, Kiss O. Cardiopulmonary examinations of athletes returning to high-intensity sport activity following SARS-CoV-2 infection. Sci Rep. 2022;12(1):21686.

67. Valle C, Ujvari A, Elia E, Lu M, Gauthier N, Hoganson D, Marx G, Powell AJ, Ferraro A, Lakatos B, Toser Z, Merkely B, Kovacs A, Harrild DM. Right ventricular contraction patterns in healthy children using three-dimensional echocardiography. Front Cardiovasc Med. 2023;10:1141027.

68. Ujvari A, Fabian A, Lakatos B, Tokodi M, Ladanyi Z, Sydo N, Csulak E, Vago H, Juhasz V, Grebur K, Szucs A, Zamodics M, Babity M, Kiss O, Merkely B, Kovacs A. Right Ventricular Structure and Function in Adolescent Athletes: A 3D Echocardiographic Study. Int J Sports Med. 2024;45(6):473-80.

69. Antoni ML, Scherptong RW, Atary JZ, Boersma E, Holman ER, van der Wall EE, Schalij MJ, Bax JJ. Prognostic value of right ventricular function in patients after acute myocardial infarction treated with primary percutaneous coronary intervention. Circ Cardiovasc Imaging. 2010;3(3):264-71.

70. Carluccio E, Biagioli P, Alunni G, Murrone A, Zuchi C, Coiro S, Riccini C, Mengoni A, D'Antonio A, Ambrosio G. Prognostic Value of Right Ventricular Dysfunction in Heart Failure With Reduced Ejection Fraction: Superiority of Longitudinal Strain Over Tricuspid Annular Plane Systolic Excursion. Circ Cardiovasc Imaging. 2018;11(1):e006894.

71. Amsallem M, Sweatt AJ, Aymami MC, Kuznetsova T, Selej M, Lu H, Mercier O, Fadel E, Schnittger I, McConnell MV, Rabinovitch M, Zamanian RT, Haddad F. Right Heart End-Systolic Remodeling Index Strongly Predicts Outcomes in Pulmonary Arterial Hypertension: Comparison With Validated Models. Circ Cardiovasc Imaging. 2017;10(6).

72. Spiewak M, Malek LA, Petryka J, Mazurkiewicz L, Werys K, Biernacka EK, Kowalski M, Hoffman P, Demkow M, Misko J, Ruzyllo W. Repaired tetralogy of Fallot: ratio of right ventricular volume to left ventricular volume as a marker of right ventricular dilatation. Radiology. 2012;265(1):78-86.

73. Nagata Y, Wu VC, Kado Y, Otani K, Lin FC, Otsuji Y, Negishi K, Takeuchi M. Prognostic Value of Right Ventricular Ejection Fraction Assessed by Transthoracic 3D Echocardiography. Circ Cardiovasc Imaging. 2017;10(2).

74. Kovacs A, Lakatos B, Tokodi M, Merkely B. Right ventricular mechanical pattern in health and disease: beyond longitudinal shortening. Heart Fail Rev. 2019;24(4):511-20.

75. Kjaergaard J, Akkan D, Iversen KK, Kober L, Torp-Pedersen C, Hassager C. Right ventricular dysfunction as an independent predictor of short- and long-term mortality in patients with heart failure. Eur J Heart Fail. 2007;9(6-7):610-6.

76. Merlo M, Gobbo M, Stolfo D, Losurdo P, Ramani F, Barbati G, Pivetta A, Di Lenarda A, Anzini M, Gigli M, Pinamonti B, Sinagra G. The Prognostic Impact of the Evolution of RV Function in Idiopathic DCM. JACC Cardiovasc Imaging. 2016;9(9):1034-42.

77. Lakatos B, Toser Z, Tokodi M, Doronina A, Kosztin A, Muraru D, Badano LP, Kovacs A, Merkely B. Quantification of the relative contribution of the different right ventricular wall motion components to right ventricular ejection fraction: the ReVISION method. Cardiovasc Ultrasound. 2017;15(1):8.

78. Maffessanti F, Muraru D, Esposito R, Gripari P, Ermacora D, Santoro C, Tamborini G, Galderisi M, Pepi M, Badano LP. Age-, body size-, and sex-specific reference values for right ventricular volumes and ejection fraction by three-dimensional echocardiography: a multicenter echocardiographic study in 507 healthy volunteers. Circ Cardiovasc Imaging. 2013;6(5):700-10.

79. Addetia K, Muraru D, Badano LP, Lang RM. New Directions in Right Ventricular Assessment Using 3-Dimensional Echocardiography. JAMA Cardiol. 2019;4(9):936-44.

80. Santamore WP, Gray L, Jr. Significant left ventricular contributions to right ventricular systolic function. Mechanism and clinical implications. Chest. 1995;107(4):1134-45.

81. Kind T, Mauritz GJ, Marcus JT, van de Veerdonk M, Westerhof N, Vonk-Noordegraaf A. Right ventricular ejection fraction is better reflected by transverse rather than longitudinal wall motion in pulmonary hypertension. J Cardiovasc Magn Reson. 2010;12(1):35.

82. Sakuma M, Ishigaki H, Komaki K, Oikawa Y, Katoh A, Nakagawa M, Hozawa H, Yamamoto Y, Takahashi T, Shirato K. Right ventricular ejection function assessed by cineangiography--Importance of bellows action. Circ J. 2002;66(6):605-9.

83. Greyson CR. The right ventricle and pulmonary circulation: basic concepts. Rev Esp Cardiol. 2010;63(1):81-95.

84. Moceri P, Duchateau N, Baudouy D, Schouver ED, Leroy S, Squara F, Ferrari E, Sermesant M. Three-dimensional right-ventricular regional deformation and survival in pulmonary hypertension. Eur Heart J Cardiovasc Imaging. 2018;19(4):450-8.

85. Ishizu T, Seo Y, Atsumi A, Tanaka YO, Yamamoto M, Machino-Ohtsuka T, Horigome H, Aonuma K, Kawakami Y. Global and Regional Right Ventricular Function Assessed by Novel Three-Dimensional Speckle-Tracking Echocardiography. J Am Soc Echocardiogr. 2017;30(12):1203-13.

86. Stokke TM, Hasselberg NE, Smedsrud MK, Sarvari SI, Haugaa KH, Smiseth OA, Edvardsen T, Remme EW. Geometry as a Confounder When Assessing Ventricular

Systolic Function: Comparison Between Ejection Fraction and Strain. J Am Coll Cardiol. 2017;70(8):942-54.

87. Muraru D, Onciul S, Peluso D, Soriani N, Cucchini U, Aruta P, Romeo G, Cavalli G, Iliceto S, Badano LP. Sex- and Method-Specific Reference Values for Right Ventricular Strain by 2-Dimensional Speckle-Tracking Echocardiography. Circ Cardiovasc Imaging. 2016;9(2):e003866.

88. Chia EM, Hsieh CH, Boyd A, Pham P, Vidaic J, Leung D, Thomas L. Effects of age and gender on right ventricular systolic and diastolic function using two-dimensional speckle-tracking strain. J Am Soc Echocardiogr. 2014;27(10):1079-86 e1.

89. Sanchez-Quintana D, Garcia-Martinez V, Climent V, Hurle JM. Morphological changes in the normal pattern of ventricular myoarchitecture in the developing human heart. Anat Rec. 1995;243(4):483-95.

90. Lakatos BK, Tokodi M, Assabiny A, Toser Z, Kosztin A, Doronina A, Racz K, Koritsanszky KB, Berzsenyi V, Nemeth E, Sax B, Kovacs A, Merkely B. Dominance of free wall radial motion in global right ventricular function of heart transplant recipients. Clin Transplant. 2018;32(3):e13192.

91. Cho EJ, Jiamsripong P, Calleja AM, Alharthi MS, McMahon EM, Khandheria BK, Belohlavek M. Right ventricular free wall circumferential strain reflects graded elevation in acute right ventricular afterload. Am J Physiol Heart Circ Physiol. 2009;296(2):H413-20.

92. Lam CS, Borlaug BA, Kane GC, Enders FT, Rodeheffer RJ, Redfield MM. Age-associated increases in pulmonary artery systolic pressure in the general population. Circulation. 2009;119(20):2663-70.

93. Gorter TM, van Veldhuisen DJ, Bauersachs J, Borlaug BA, Celutkiene J, Coats AJS, Crespo-Leiro MG, Guazzi M, Harjola VP, Heymans S, Hill L, Lainscak M, Lam CSP, Lund LH, Lyon AR, Mebazaa A, Mueller C, Paulus WJ, Pieske B, Piepoli MF, Ruschitzka F, Rutten FH, Seferovic PM, Solomon SD, Shah SJ, Triposkiadis F, Wachter R, Tschope C, de Boer RA. Right heart dysfunction and failure in heart failure with preserved ejection fraction: mechanisms and management. Position statement on behalf of the Heart Failure Association of the European Society of Cardiology. Eur J Heart Fail. 2018;20(1):16-37.

94. Wink J, de Wilde RB, Wouters PF, van Dorp EL, Veering BT, Versteegh MI, Aarts LP, Steendijk P. Thoracic Epidural Anesthesia Reduces Right Ventricular Systolic Function With Maintained Ventricular-Pulmonary Coupling. Circulation. 2016;134(16):1163-75.

95. Zanobini M, Saccocci M, Tamborini G, Veglia F, Di Minno A, Poggio P, Pepi M, Alamanni F, Loardi C. Postoperative Echocardiographic Reduction of Right Ventricular Function: Is Pericardial Opening Modality the Main Culprit? Biomed Res Int. 2017;2017:4808757.

96. Addetia K, Miyoshi T, Amuthan V, Citro R, Daimon M, Gutierrez Fajardo P, Kasliwal RR, Kirkpatrick JN, Monaghan MJ, Muraru D, Ogunyankin KO, Park SW, Ronderos RE, Sadeghpour A, Scalia GM, Takeuchi M, Tsang W, Tucay ES, Tude Rodrigues AC, Zhang Y, Singulane CC, Hitschrich N, Blankenhagen M, Degel M, Schreckenberg M, Mor-Avi V, Asch FM, Lang RM, Investigators W. Normal Values of Three-Dimensional Right Ventricular Size and Function Measurements: Results of the World Alliance Societies of Echocardiography Study. J Am Soc Echocardiogr. 2023;36(8):858-66 e1.

97. Asch FM, Banchs J, Price R, Rigolin V, Thomas JD, Weissman NJ, Lang RM. Need for a Global Definition of Normative Echo Values-Rationale and Design of the World Alliance of Societies of Echocardiography Normal Values Study (WASE). J Am Soc Echocardiogr. 2019;32(1):157-62 e2.

98. Reddy YNV, Anantha-Narayanan M, Obokata M, Koepp KE, Erwin P, Carter RE, Borlaug BA. Hemodynamic Effects of Weight Loss in Obesity: A Systematic Review and Meta-Analysis. JACC Heart Fail. 2019;7(8):678-87.

99. Vasan RS. Cardiac function and obesity. Heart. 2003;89(10):1127-9.

100. Woodard JC, Chow E, Farrar DJ. Isolated ventricular systolic interaction during transient reductions in left ventricular pressure. Circ Res. 1992;70(5):944-51.

101. Mulieri LA, Tischler MD, Martin BJ, Leavitt BJ, Ittleman FP, Alpert NR, LeWinter MM. Regional differences in the force-frequency relation of human left ventricular myocardium in mitral regurgitation: implications for ventricular shape. Am J Physiol Heart Circ Physiol. 2005;288(5):H2185-91.

102. Hauck A, Guo R, Ivy DD, Younoszai A. Tricuspid annular plane systolic excursion is preserved in young patients with pulmonary hypertension except when associated with repaired congenital heart disease. Eur Heart J Cardiovasc Imaging. 2017;18(4):459-66.
103. Lianza AC, Rodrigues ACT, Mercer-Rosa L, Vieira MLC, de Oliveira WAA, Afonso TR, Nomura CH, da Silva JP, da Silva LDF, Szarf G, Tavares GMP, Fischer CH, Morhy SS. Right Ventricular Systolic Function After the Cone Procedure for Ebstein's Anomaly: Comparison Between Echocardiography and Cardiac Magnetic Resonance. Pediatr Cardiol. 2020;41(5):985-95.
104. Levy PT, El-Khuffash A, Patel MD, Breatnach CR, James AT, Sanchez AA, Abuchabe C, Rogal SR, Holland MR, McNamara PJ, Jain A, Franklin O, Mertens L, Hamvas A, Singh GK. Maturational Patterns of Systolic Ventricular Deformation Mechanics by Two-Dimensional Speckle-Tracking Echocardiography in Preterm Infants over the First Year of Age. J Am Soc Echocardiogr. 2017;30(7):685-98 e1.
105. Surkova E, Kovacs A, Tokodi M, Lakatos BK, Merkely B, Muraru D, Ruocco A, Parati G, Badano LP. Contraction Patterns of the Right Ventricle Associated with Different Degrees of Left Ventricular Systolic Dysfunction. Circ Cardiovasc Imaging. 2021;14(10):e012774.
106. Surkova E, Kovacs A, Lakatos BK, Tokodi M, Fabian A, West C, Senior R, Li W. Contraction patterns of the systemic right ventricle: a three-dimensional echocardiography study. Eur Heart J Cardiovasc Imaging. 2022;23(12):1654-62.
107. Bhatt SM, Wang Y, Elci OU, Goldmuntz E, McBride M, Paridon S, Mercer-Rosa L. Right Ventricular Contractile Reserve Is Impaired in Children and Adolescents With Repaired Tetralogy of Fallot: An Exercise Strain Imaging Study. J Am Soc Echocardiogr. 2019;32(1):135-44.
108. Maskatia SA, Petit CJ, Travers CD, Goldberg DJ, Rogers LS, Glatz AC, Qureshi AM, Goldstein BH, Ao J, Sachdeva R. Echocardiographic parameters associated with biventricular circulation and right ventricular growth following right ventricular decompression in patients with pulmonary atresia and intact ventricular septum: Results from a multicenter study. Congenit Heart Dis. 2018;13(6):892-902.
109. Bidviene J, Muraru D, Maffessanti F, Ereminiene E, Kovacs A, Lakatos B, Vaskelyte JJ, Zaliunas R, Surkova E, Parati G, Badano LP. Regional shape, global function and mechanics in right ventricular volume and pressure overload conditions: a

three-dimensional echocardiography study. Int J Cardiovasc Imaging. 2021;37(4):1289-99.

110. McClean G, Riding NR, Ardern CL, Farooq A, Pieles GE, Watt V, Adamuz C, George KP, Oxborough D, Wilson MG. Electrical and structural adaptations of the paediatric athlete's heart: a systematic review with meta-analysis. Br J Sports Med. 2018;52(4):230.

111. Churchill TW, Groezinger E, Loomer G, Baggish AL. Exercise-induced cardiac remodeling during adolescence. Eur J Prev Cardiol. 2020;27(19):2148-50.

112. Bjerring AW, Landgraff HE, Stokke TM, Murbraech K, Leirstein S, Aaeng A, Brun H, Haugaa KH, Hallen J, Edvardsen T, Sarvari SI. The developing athlete's heart: a cohort study in young athletes transitioning through adolescence. Eur J Prev Cardiol. 2019;26(18):2001-8.

113. Styne DM. The regulation of pubertal growth. Horm Res. 2003;60(Suppl 1):22-6.

114. Hietalampi H, Pahkala K, Jokinen E, Ronnemaa T, Viikari JS, Niinikoski H, Heinonen OJ, Salo P, Simell O, Raitakari OT. Left ventricular mass and geometry in adolescence: early childhood determinants. Hypertension. 2012;60(5):1266-72.

115. Olah A, Kovacs A, Lux A, Tokodi M, Braun S, Lakatos BK, Matyas C, Kellermayer D, Ruppert M, Sayour AA, Barta BA, Merkely B, Radovits T. Characterization of the dynamic changes in left ventricular morphology and function induced by exercise training and detraining. Int J Cardiol. 2019;277:178-85.

116. D'Ascenzi F, Pelliccia A, Valentini F, Malandrino A, Natali BM, Barbati R, Focardi M, Bonifazi M, Mondillo S. Training-induced right ventricular remodelling in pre-adolescent endurance athletes: The athlete's heart in children. Int J Cardiol. 2017;236:270-5.

117. Rundqvist L, Engvall J, Faresjo M, Carlsson E, Blomstrand P. Regular endurance training in adolescents impacts atrial and ventricular size and function. Eur Heart J Cardiovasc Imaging. 2017;18(6):681-7.

118. Gomez AD, Zou H, Bowen ME, Liu X, Hsu EW, McKellar SH. Right Ventricular Fiber Structure as a Compensatory Mechanism in Pressure Overload: A Computational Study. J Biomech Eng. 2017;139(8):0810041-08100410.

119. Jone PN, Le L, Pan Z, Goot BH, Parthiban A, Harrild D, Ferraro AM, Marx G, Colen T, Khoo NS. Three-Dimensional Echocardiography Right Ventricular Volumes and

Ejection Fraction Reference Values in Children: A North American Multicentre Study. Can J Cardiol. 2022;38(9):1426-33.
120. Fabian A, Lakatos BK, Tokodi M, Kiss AR, Sydo N, Csulak E, Kispal E, Babity M, Szucs A, Kiss O, Merkely B, Kovacs A. Geometrical remodeling of the mitral and tricuspid annuli in response to exercise training: a 3-D echocardiographic study in elite athletes. Am J Physiol Heart Circ Physiol. 2021;320(5):H1774-H85.
121. Doronina A, Edes IF, Ujvari A, Kantor Z, Lakatos BK, Tokodi M, Sydo N, Kiss O, Abramov A, Kovacs A, Merkely B. The Female Athlete's Heart: Comparison of Cardiac Changes Induced by Different Types of Exercise Training Using 3D Echocardiography. Biomed Res Int. 2018;2018:3561962.
122. Kovacs A, Apor A, Nagy A, Vago H, Toth A, Nagy AI, Kovats T, Sax B, Szeplaki G, Becker D, Merkely B. Left ventricular untwisting in athlete's heart: key role in early diastolic filling? Int J Sports Med. 2014;35(3):259-64.

9. BIBLIOGRAPHY OF THE CANDIDATE

9.1. Bibliography related to the present thesis

1. Lakatos BK, Nabeshima Y, Tokodi M, Nagata Y, Tősér Z, Otani K, Kitano T, Fábián A, **Ujvári A**, Boros AM, Merkely B, Kovács A, Takeuchi M. Importance of Nonlongitudinal Motion Components in Right Ventricular Function: Three-Dimensional Echocardiographic Study in Healthy Volunteers. *J Am Soc Echocardiogr*. 2020;33:995-1005.e1001. doi: 10.1016/j.echo.2020.04.002.
   IF: 5,251

2. Valle C, **Ujvari A** *, Elia E, Lu M, Gauthier N, Hoganson D, Marx G, Powell AJ, Ferraro A, Lakatos B, Tősér Z, Merkely B, Kovács A, Harrild DM. Right ventricular contraction patterns in healthy children using three-dimensional echocardiography. *Front Cardiovasc Med*. 2023;10:1141027. doi: 10.3389/fcvm.2023.1141027.
   IF: 2,76
   * Shared first authorship

3. **Ujvari A**, Fabian A, Lakatos B, Tokodi M, Ladanyi Z, Sydo N, Csulak E, Vago H, Juhasz V, Grebur K, Szucs A, Zamodics M, Babity M, Kiss O, Merkely B, Kovacs A. Right Ventricular Structure and Function in Adolescent Athletes: A 3D Echocardiographic Study. *Int J Sports Med*. 2024. doi: 10.1055/a-2259-2203.
   IF: 2,0

9.2. Bibliography not related to the present thesis

1. Ladanyi Z, Balint T, Fabian A, **Ujvari A**, Turschl TK, Nagy D, Straub E, Fejer Cs, Zima E, Apor A, Nagy AI, Szigethi T, Papp R, Molnar L, Kovacs A, Ruppert M, Lakatos BK, Merkely B. Non-invasive myocardial work as an independent predictor of postprocedural NT-proBNP in elderly patients undergoing transcatheter aortic valve replacement. *GeroScience*. 2025. 47, 3311–3323.doi:10.1007/s11357-024-01302-0.
   IF: 5,4

2. Zamodics M, Babity M, Schay G, Leel-Ossy T, Bucsko-Varga A, Kulcsar P, Benko R, Boroncsok D, Fabian A, **Ujvari A**, Ladanyi Zs, Balla D, Vago H, Kovacs A, Hosszu E, Meszaros Sz, Horvath Cs, Merkely B, Kiss O. Correlations Between Body Composition and Aerobic Fitness in Elite Female Youth Water Polo Players. *Sports(Basel)*.2025;13(2):51.doi:10.3390/sports13020051.
IF: 2,9

3. Ladanyi Z, Eltayeb A, Fabian A, **Ujvari A**, Tolvaj M, Tokodi M, Choudhary KA, Kovacs A, Merkely B, Vriz O, Lakatos BK. The effects of mitral stenosis on right ventricular mechanics assessed by three-dimensional echocardiography. *Sci Rep*.2024;14(1):17112.doi:10.1038/s41598-024-68126-y.
IF: 3,9

4. Ladanyi Z, Barczi A, Fabian A, **Ujvari A**, Cseprekal O, Kis E, Reusz GS, Kovacs A, Merkely B, Lakatos BK. Get to the heart of pediatric kidney transplant recipients: Evaluation of left- and right ventricular mechanics by three-dimensional echocardiography. *Front Cardiovasc Med*. 2023;10:1094765. doi: 10.3389/fcvm.2023.1094765.
IF: 2,76

5. Fabian A, **Ujvari A**, Tokodi M, Lakatos BK, Kiss O, Babity M, Zamodics M, Sydo N, Csulak E, Vago H, Szabo L, Kiss AR, Szucs A, Hizoh I, Merkely B, Kovacs A. Biventricular mechanical pattern of the athlete's heart: comprehensive characterization using three-dimensional echocardiography. *Eur J Prev Cardiol*. 2022;29:1594-1604. doi: 10.1093/eurjpc/zwac026.
IF: 8,3

6. **Ujvari A**, Lakatos BK, Tokodi M, Fabian A, Merkely B, Kovacs A. Evaluation of Left Ventricular Structure and Function using 3D Echocardiography. *J Vis Exp*. 2020. doi: 10.3791/61212.
IF: 1,36

7. Doronina A, Edes IF, **Ujvari A**, Kantor Z, Lakatos BK, Tokodi M, Sydo N, Kiss O, Abramov A, Kovacs A, Merkely B. The Female Athlete's Heart: Comparison of Cardiac Changes Induced by Different Types of Exercise Training Using 3D Echocardiography. *Biomed Res Int*. 2018;2018:3561962. doi: 10.1155/2018/3561962.
IF: 2,197

9.3. Hungarian journal articles

1. Kai S, **Ujvári A**, Lakatos B, Tokodi M, Kosztin A, Veres B, Schwertner WR, Kovács A, Fábián A, Merkely BP. (2022) Tricuspid regurgiatition and right ventricular contraction pattern in heart failure with reduced ejection fraction: a 3D echocardiography study. CARDIOLOGIA HUNGARICA, 52: 14-22.

2. Tolvaj M, Tokodi M, Lakatos B, Fábián A, **Ujvári A**, Zhubi Bakija F, Ladányi Z, Tarcza Z, Merkely BP, Kovács A. (2021) Added predictive value of right ventricular ejection fraction compared with conventional echocardiographic measurements in patients who underwent diverse cardiovascular procedures. IMAGING, 13: 130-137.

3. Parázs N, Lakatos BK, Kovács A, Assabiny A, Király Á, Tarjányi Z, Szakál-Tóth Zs, Teszák T, Tokodi M, **Ujvári A**, Kugler Sz, Szűcs N, Merkely B, Sax B. Jobbszívfél-elégtelenség évekkel a szívtranszplantációt követően : Egy ritka etiológiai tényező esete. CARDIOLOGIA HUNGARICA 51 pp. 69-72. , 4 p. (2021)

4. Kántor Z, Lakatos BK, Kiss O, Sydó N, Tokodi M, Vágó H, Csécs I, **Ujvári A**, Fábián A, Babity M, Kovács A, Merkely B. A bal kamra globális és szegmentális deformációjának jellemzése speckle-tracking echokardiográfiával fiatal sportolókban. CARDIOLOGIA HUNGARICA 49 : Suppl. B pp. B115-B116. (2019)

5. **Ujvári A**, Komka Zs, Kántor Z, Lakatos BK, Tokodi Márton, Doronina A, Babity M, Bognár Cs, Kiss O, Merkely B, Kovács A. Kajakos és kenus élsportolók bal és jobb kamrai analízise 3D echokardiográfia segítségével. CARDIOLOGIA HUNGARICA 48 : 1 pp. 13-19. , 7 p. (2018)

10. ACKNOWLEDGEMENTS

This present thesis and the previous work would not have been possible without the tremendous amount of help and support that I received from several people. First and foremost, I am exceptionally grateful to my supervisor and mentor, Dr. Attila Kovács for letting me become a part of his extremely talented work group. I sincerely appreciate your invaluable guidance, counsel, and unwavering belief in my abilities from the beginning. Your wealth of experience and expertise in clinical cardiology and research has been a constant source of motivation for me and will undoubtedly continue to influence my career trajectory.

I would like to also express my sincere gratitude towards Professor Béla Merkely for his professional guidance, and for creating an exceptional scientific institution and providing outstanding opportunities for my PhD research.

I am incredibly grateful for all the members of and co-workers of the Department of Sports Cardiology and the Echocardiography Working Group for their arduous work and their valuable insights, which were substantial for my scientific projects.

Many thanks to all the PhD students and colleagues: Dr. Alexandra Fábián, Dr. Bálint Lakatos, Dr. Márton Tokodi, Dr. Zsuzsanna Ladányi, Dr. Máté Tolvaj, Ádám Szijártó, and also to all of the co-workers at the Heart and Vascular Center for their immense contribution and help.

Finally, I am overwhelmed with gratitude towards my parents and family for providing a supportive, and affectionate environment. Words cannot express the depth of my appreciation, but I will try anyways: thank you for your unwavering support, without you, none of this would have been possible.